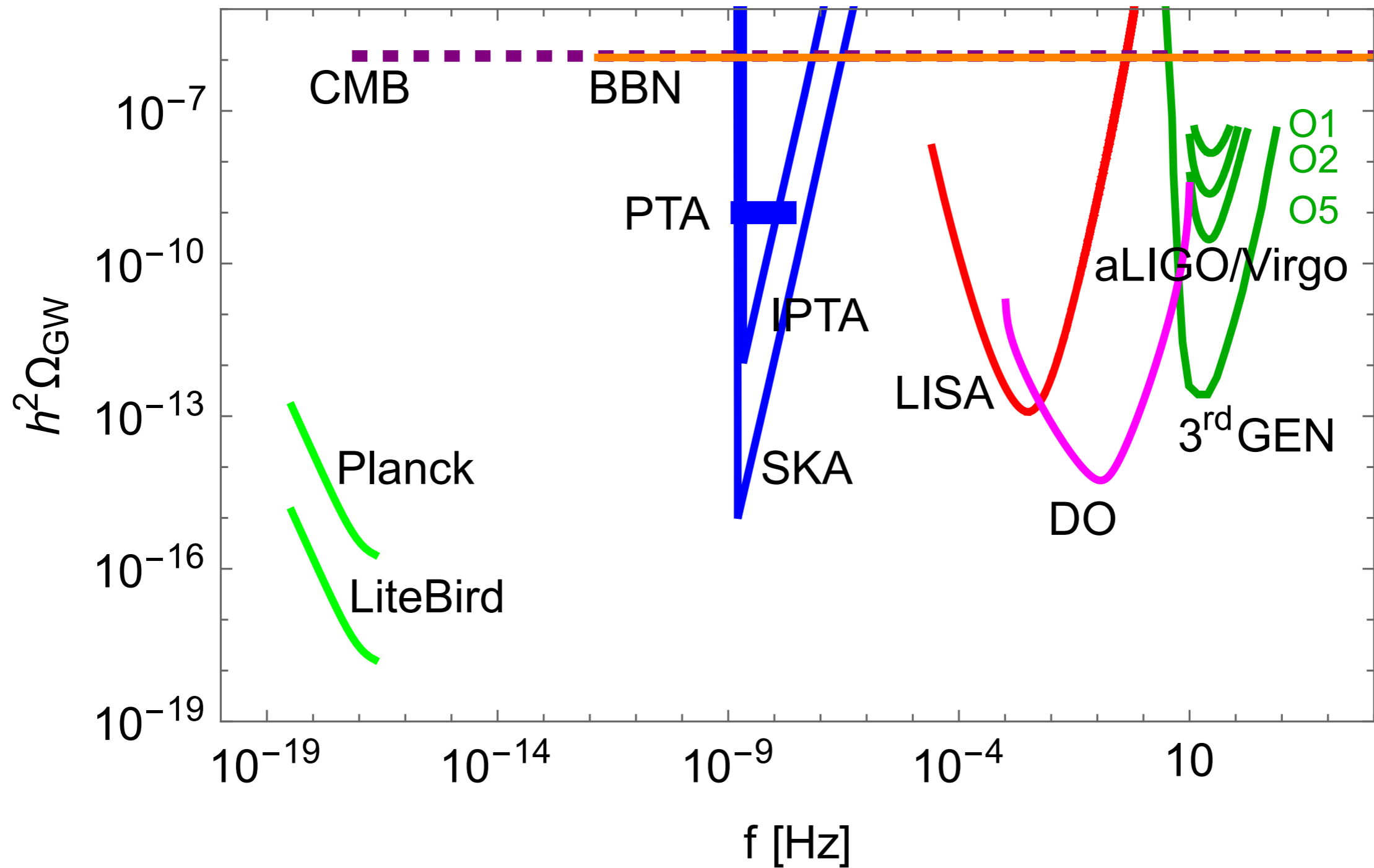


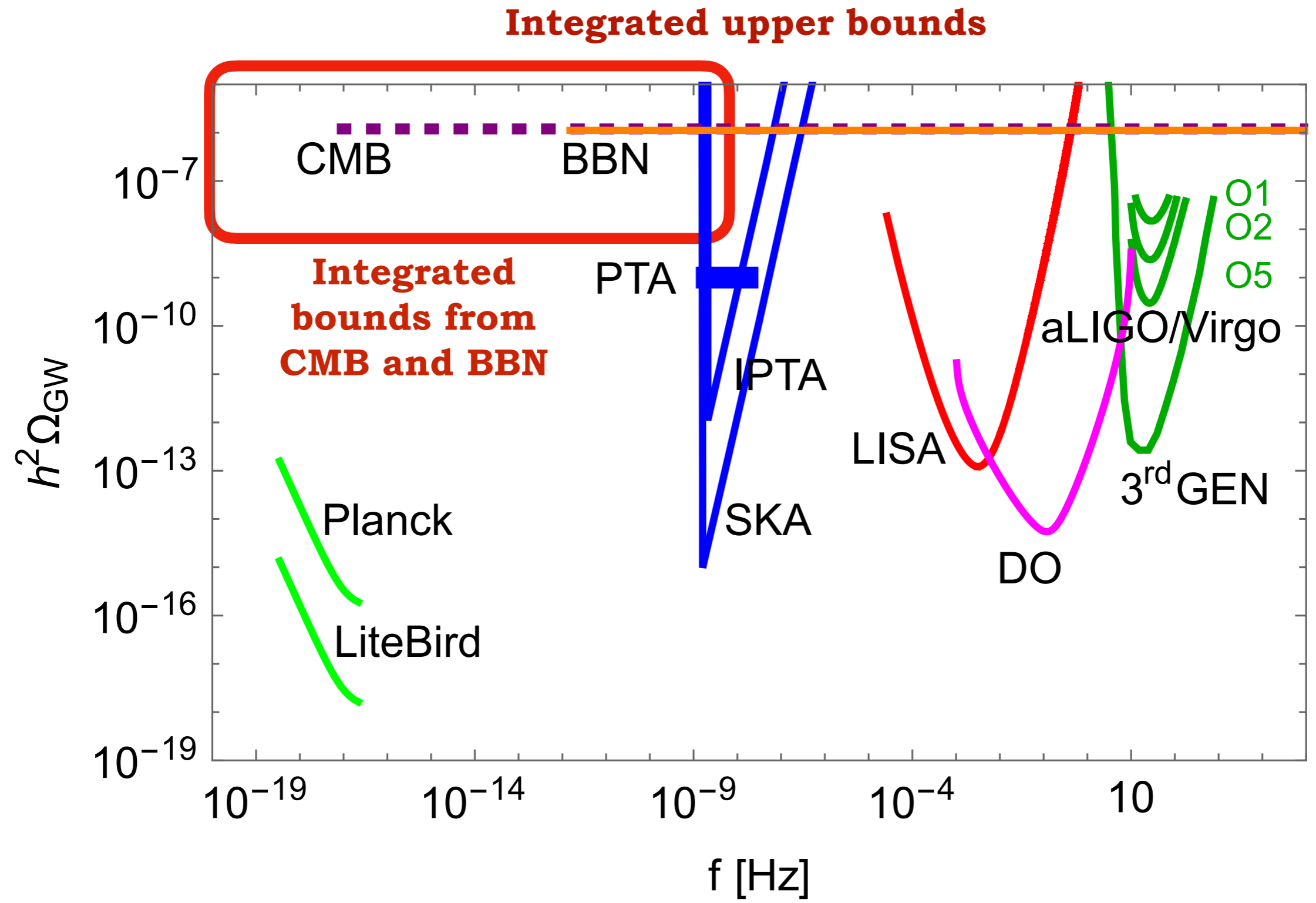
# Astrophysical and cosmological aspects of gravitational waves

Chiara Caprini  
University of Geneva and CERN

# What is/will be known about the SGWB



# What is/will be known about the SGWB



# What is/will be known about the SGWB

- GW contribute to the energy density in the universe and change its background evolution

$$H^2(T) = \frac{8\pi G}{3} \Sigma_i \rho_i(T)$$

- The abundances of elements produced at Big Bang Nucleosynthesis (BBN) depend on the relative abundance of neutrons and protons, which depends on the Hubble scale at  $T \sim \text{MeV}$
- The Cosmic Microwave Background (CMB) monopole and anisotropy spectrum depend on the Hubble scale at decoupling  $T \sim 0.3 \text{ eV}$ , on the matter-radiation equality...
- Bounds on the *integrated GW energy density* at/previous to the BBN and CMB epochs

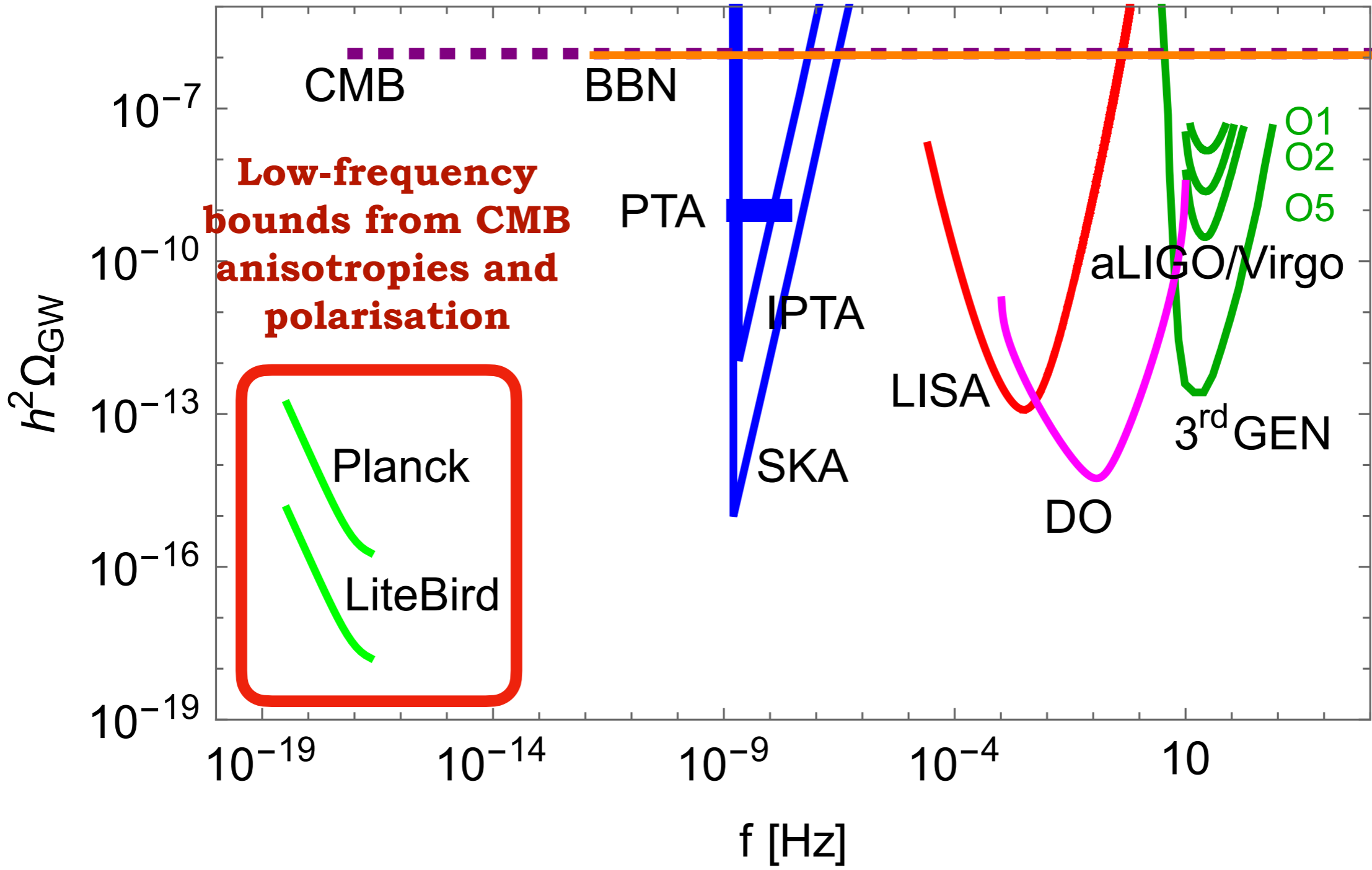
$$\left( \frac{\rho_{\text{GW}}}{\rho_c} \right)_0 = \int \frac{df}{f} \Omega_{\text{GW}}(f) = \Omega_{\gamma}^0 \left( \frac{g_S(T_0)}{g_S(T)} \right)^{4/3} \left( \frac{\rho_{\text{GW}}}{\rho_{\gamma}} \right)_T$$

CAREFUL! Plot “wrong”...



# What is/will be known about the SGWB

## CMB bounds



# Cosmic microwave background

frequency range of detection:  $10^{-18} \text{ Hz} < f < 10^{-16} \text{ Hz}$

- **temperature anisotropy:**  
limit by Planck

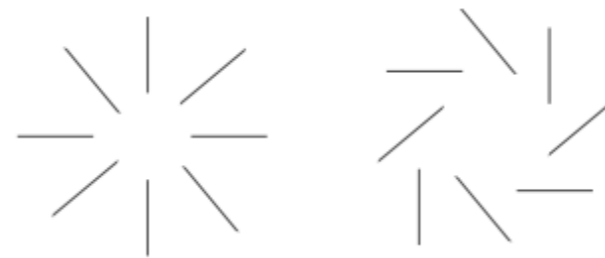
$$\frac{\delta T}{T} = - \int_{t_{\text{dec}}}^{t_0} \dot{h}_{ij} n^i n^j dt$$

$$P_h(k) = A_t(k_0) (k \eta_0)^{n_t} \quad C_{\ell, T}^{\Theta\Theta} \simeq \frac{\sqrt{\pi}}{3} A_t(k_0) \frac{\ell(\ell+2)!}{(\ell-2)!} \frac{\Gamma[\frac{7-n_t}{2}] \Gamma[\ell + \frac{n_t}{2}]}{\Gamma[4 - \frac{n_t}{2}] \Gamma[\ell + 7 - \frac{n_t}{2}]}$$

$$\propto \ell^{n_t-2} \quad \text{for } 1 \ll \ell \lesssim 60$$

- **polarisation:** BB spectrum measured by BICEP2 and Planck generated at photon decoupling time, from Thomson scattering of electrons by a **quadrupole temperature anisotropy** in the photons

polarisation patterns



generated by  
primordial scalar  
and tensor  
perturbations



E mode

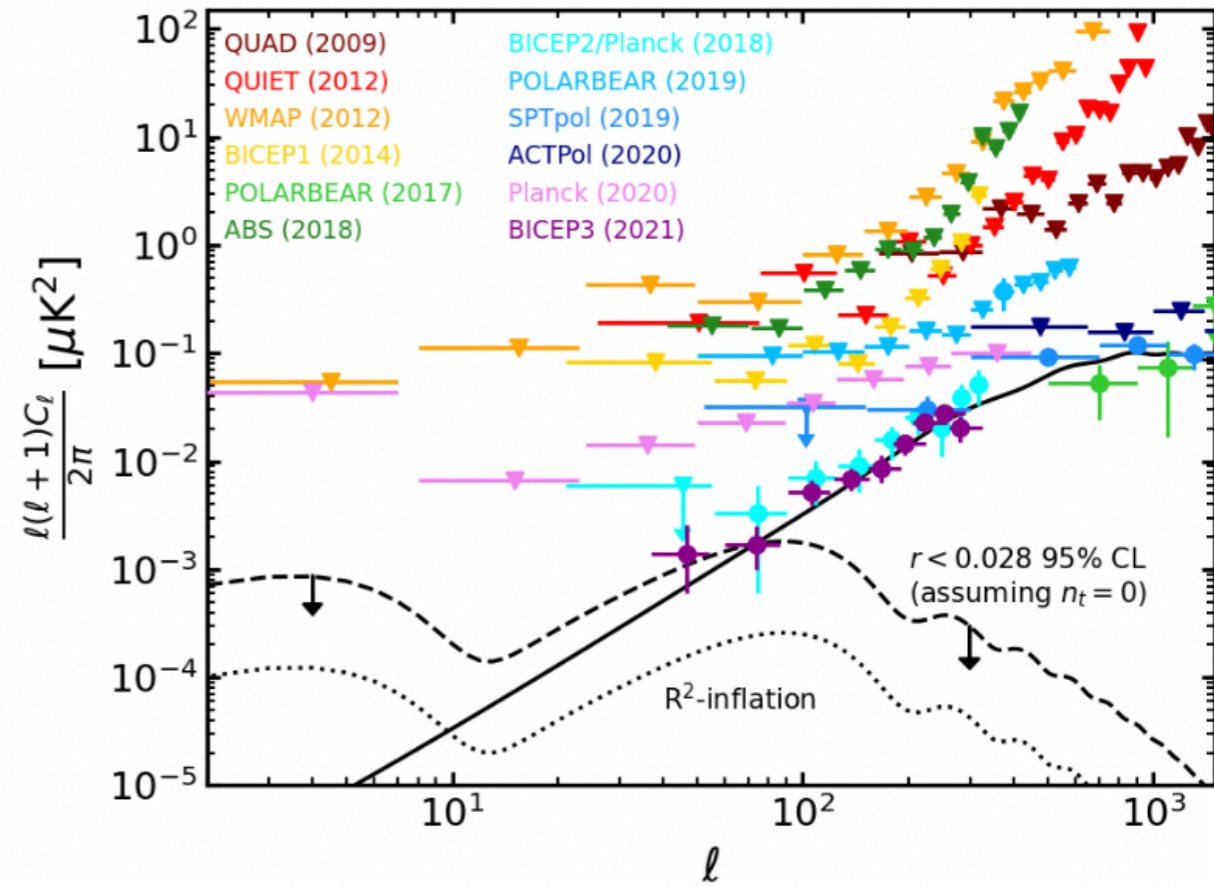
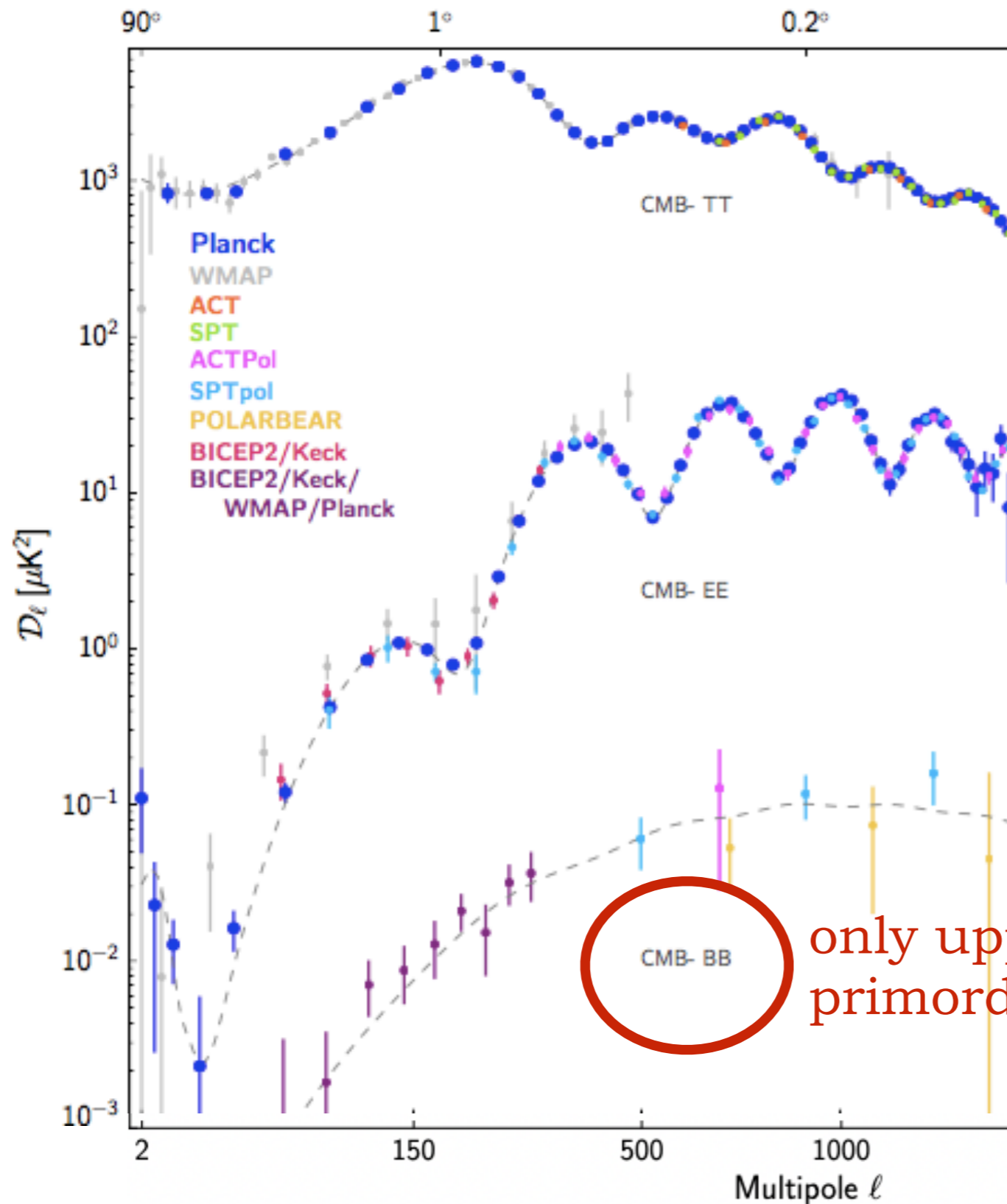


B mode

generated only by  
primordial tensor  
perturbations or by  
foregrounds

# Cosmic microwave background

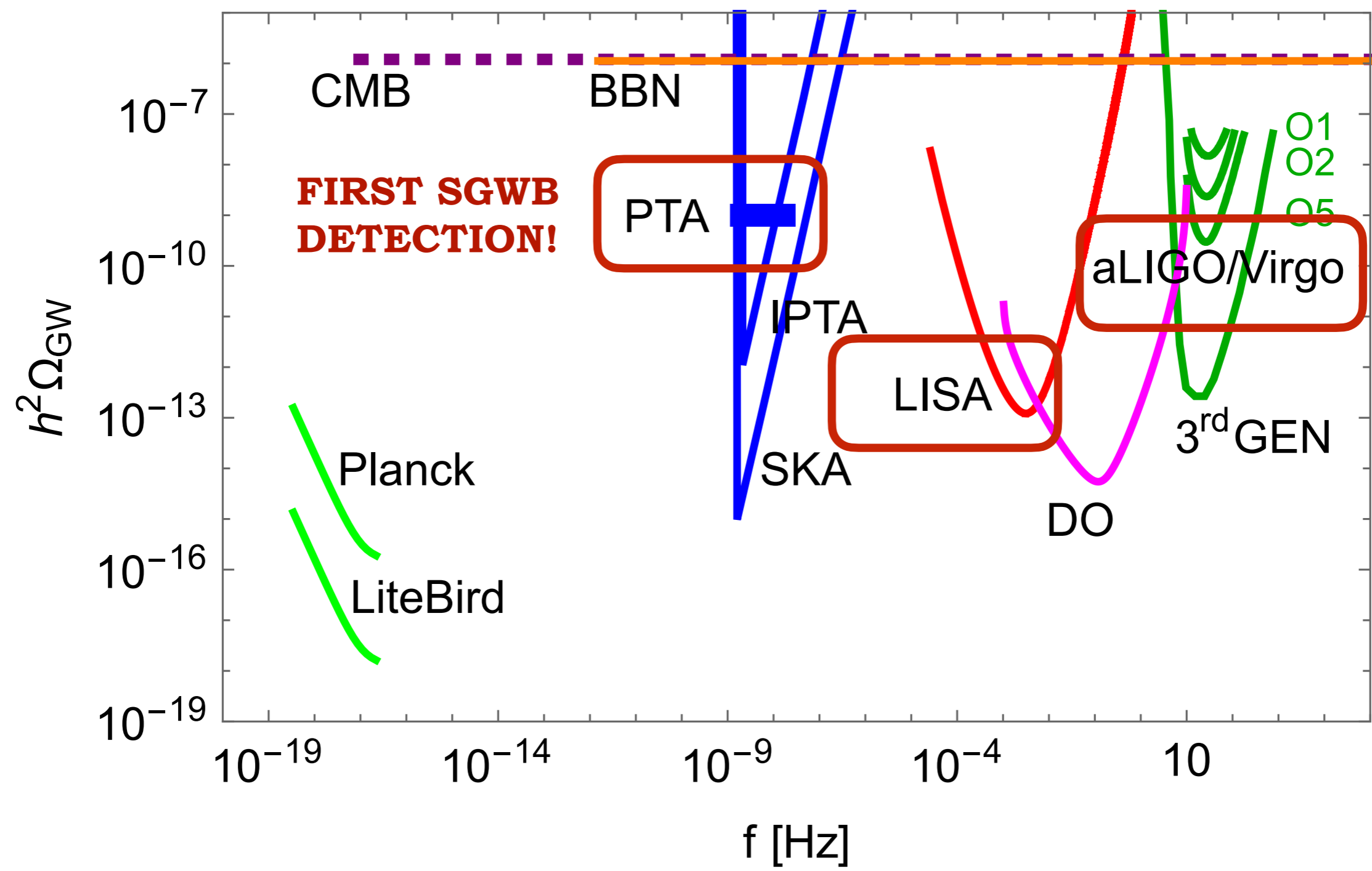
Galloni et al: arXiv:2208.00188



only upper bounds on the primordial component for now

# What is/will be known about the SGWB

## Present and future GW observatories





# Earth-based interferometers

aLIGO/aVirgo (operating)

arm length  $L = 4$  km

frequency range of detection:  
 $10 \text{ Hz} < f < 5 \text{ kHz}$

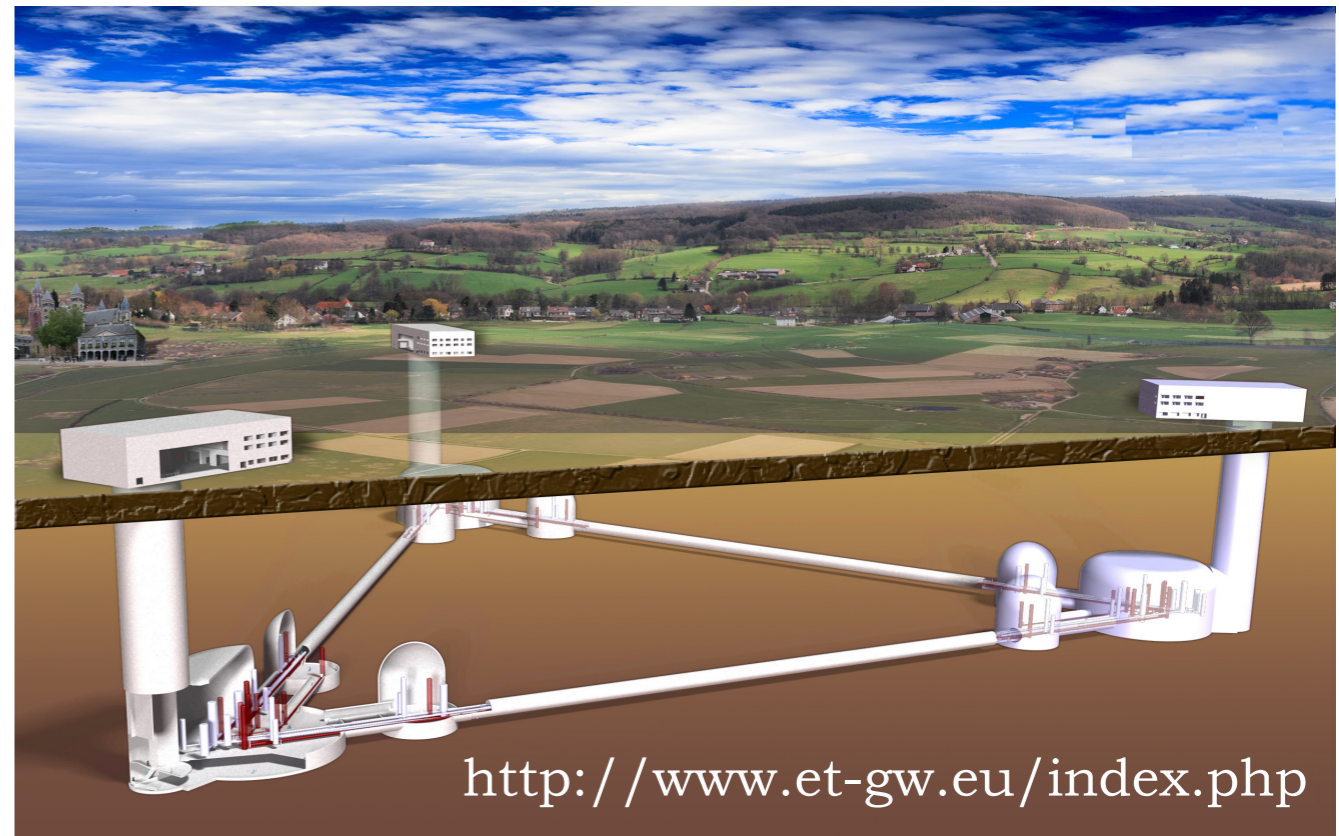
## DETECTION TARGETS:

- Black hole coalescing binaries of masses few to hundred solar masses (BHBs)
- Neutron Star and NS-BH binaries / SN explosions
- Stochastic GW background

3rd generation (ET, CE...  
coming next)

arm length  $L = 3$  km

frequency range of detection:  
 $1 \text{ Hz} < f < 10^4 \text{ HZ}$





# Earth-based interferometers

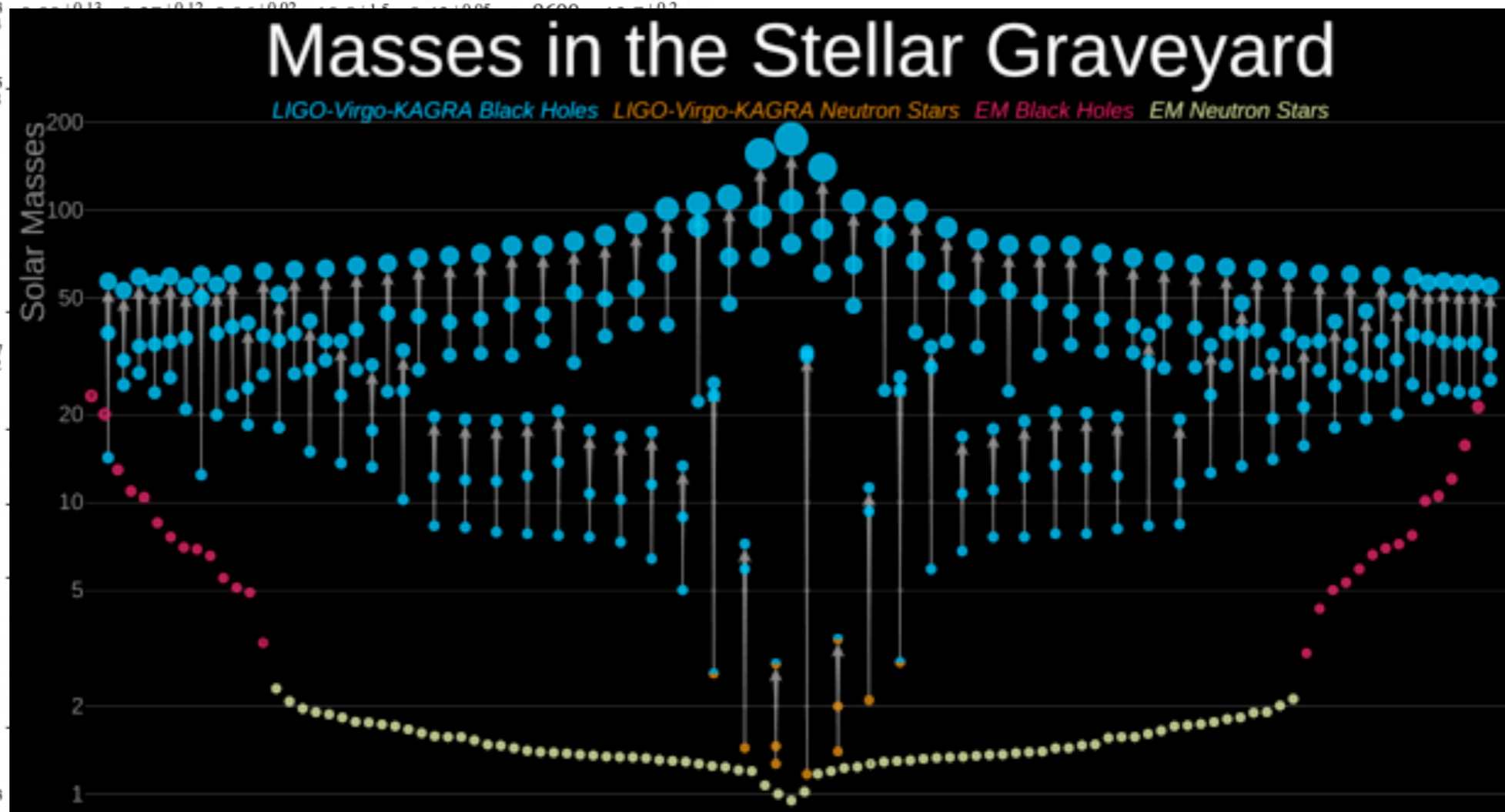
Individually resolved  
BHBs, NSBs, NS-BH

Last catalogue GWTC-3:

90 binary mergers  
detected, including NS-  
BH and NS-NS mergers

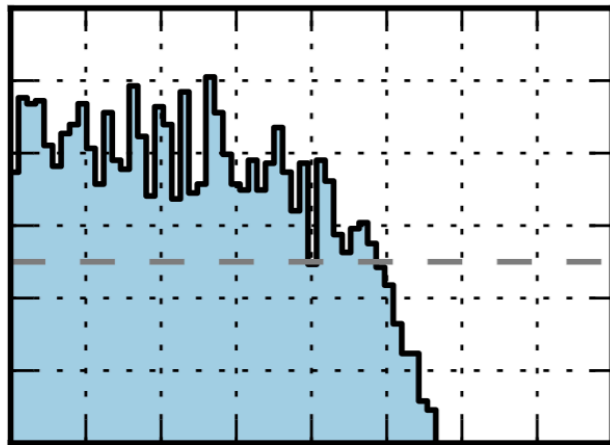
LVK Collaboration: arXiv:2111.03606

| Candidate        | $M(M_{\odot})$                          | $\mathcal{M}(M_{\odot})$               | $m_1(M_{\odot})$                      | $m_2(M_{\odot})$                       | $\chi_{\text{eff}}$                     | $D_L(\text{Gpc})$                      | $z$                                    | $M_f(M_{\odot})$                        | $\chi_f$                               | $\Delta\Omega(\text{deg}^2)$ | SNR                                  |
|------------------|---|--|---------------------------------------|--|---|--|--|---|--|------------------------------|--------------------------------------|
| GW191103_012549  | 20.0 <sup>+3.7</sup> <sub>-1.8</sub>    | 8.34 <sup>+0.66</sup> <sub>-0.57</sub> | 11.8 <sup>+6.2</sup> <sub>-2.2</sub>  | 7.9 <sup>+1.7</sup> <sub>-2.4</sub>    | 0.21 <sup>+0.16</sup> <sub>-0.10</sub>  | 0.99 <sup>+0.50</sup> <sub>-0.47</sub> | 0.20 <sup>+0.09</sup> <sub>-0.09</sub> | 19.0 <sup>+3.8</sup> <sub>-1.7</sub>    | 0.75 <sup>+0.06</sup> <sub>-0.05</sub> | 2500                         | 8.9 <sup>+0.3</sup> <sub>-0.5</sub>  |
| GW191105_143521  | 18.5 <sup>+2.1</sup> <sub>-1.3</sub>    | 7.82 <sup>+0.61</sup> <sub>-0.45</sub> | 10.7 <sup>+3.7</sup> <sub>-1.6</sub>  | 7.7 <sup>+1.4</sup> <sub>-1.9</sub>    | -0.02 <sup>+0.13</sup> <sub>-0.09</sub> | 1.15 <sup>+0.43</sup> <sub>-0.48</sub> | 0.23 <sup>+0.07</sup> <sub>-0.09</sub> | 17.6 <sup>+2.1</sup> <sub>-1.2</sub>    | 0.67 <sup>+0.04</sup> <sub>-0.05</sub> | 640                          | 9.7 <sup>+0.3</sup> <sub>-0.5</sub>  |
| GW191109_010717  | 112 <sup>+20</sup> <sub>-16</sub>       | 47.5 <sup>+9.6</sup> <sub>-7.5</sub>   | 65 <sup>+11</sup> <sub>-11</sub>      | 47 <sup>+15</sup> <sub>-13</sub>       | -0.29 <sup>+0.42</sup> <sub>-0.31</sub> | 1.29 <sup>+1.13</sup> <sub>-0.65</sub> | 0.25 <sup>+0.18</sup> <sub>-0.12</sub> | 107 <sup>+18</sup> <sub>-15</sub>       | 0.61 <sup>+0.18</sup> <sub>-0.19</sub> | 1600                         | 17.3 <sup>+0.5</sup> <sub>-0.5</sub> |
| GW191113_071753  | 34.5 <sup>+10.5</sup> <sub>-9.8</sub>   | 10.7 <sup>+1.1</sup> <sub>-1.0</sub>   | 29 <sup>+12</sup> <sub>-14</sub>      | 5.9 <sup>+4.4</sup> <sub>-1.3</sub>    | 0.00 <sup>+0.37</sup> <sub>-0.29</sub>  | 1.37 <sup>+1.15</sup> <sub>-0.62</sub> | 0.26 <sup>+0.18</sup> <sub>-0.11</sub> | 34 <sup>+11</sup> <sub>-10</sub>        | 0.45 <sup>+0.33</sup> <sub>-0.11</sub> | 3600                         | 7.9 <sup>+0.5</sup> <sub>-1.1</sub>  |
| GW191126_115259  | 20.7 <sup>+3.4</sup> <sub>-2.0</sub>    | 8.65 <sup>+0.95</sup> <sub>-0.71</sub> | 12.1 <sup>+5.5</sup> <sub>-2.2</sub>  | 8.3 <sup>+1.9</sup> <sub>-2.4</sub>    | 0.21 <sup>+0.15</sup> <sub>-0.11</sub>  | 1.62 <sup>+0.74</sup> <sub>-0.74</sub> | 0.30 <sup>+0.12</sup> <sub>-0.13</sub> | 19.6 <sup>+3.5</sup> <sub>-2.0</sub>    | 0.75 <sup>+0.06</sup> <sub>-0.05</sub> | 1400                         | 8.3 <sup>+0.2</sup> <sub>-0.5</sub>  |
| GW191127_050227  | 80 <sup>+39</sup> <sub>-22</sub>        | 29.9 <sup>+11.7</sup> <sub>-9.1</sub>  | 53 <sup>+47</sup> <sub>-20</sub>      | 24 <sup>+17</sup> <sub>-14</sub>       | 0.18 <sup>+0.34</sup> <sub>-0.36</sub>  | 3.4 <sup>+3.1</sup> <sub>-1.9</sub>    | 0.57 <sup>+0.40</sup> <sub>-0.29</sub> | 76 <sup>+39</sup> <sub>-21</sub>        | 0.75 <sup>+0.13</sup> <sub>-0.29</sub> | 980                          | 9.2 <sup>+0.7</sup> <sub>-0.6</sub>  |
| GW191129_134029  | 17.5 <sup>+2.4</sup> <sub>-1.2</sub>    | 7.31 <sup>+0.43</sup> <sub>-0.28</sub> | 10.7 <sup>+4.1</sup> <sub>-2.1</sub>  | 6.7 <sup>+1.5</sup> <sub>-1.7</sub>    | 0.06 <sup>+0.16</sup> <sub>-0.08</sub>  | 0.79 <sup>+0.26</sup> <sub>-0.33</sub> | 0.16 <sup>+0.05</sup> <sub>-0.06</sub> | 16.8 <sup>+2.5</sup> <sub>-1.2</sub>    | 0.69 <sup>+0.03</sup> <sub>-0.05</sub> | 850                          | 13.1 <sup>+0.2</sup> <sub>-0.3</sub> |
| GW191204_110529  | 47.1 <sup>+9.1</sup> <sub>-7.8</sub>    | 19.8 <sup>+3.6</sup> <sub>-3.2</sub>   | 27.3 <sup>+10.8</sup> <sub>-5.9</sub> | 19.2 <sup>+5.5</sup> <sub>-6.0</sub>   | 0.05 <sup>+0.25</sup> <sub>-0.26</sub>  | 1.9 <sup>+1.7</sup> <sub>-1.1</sub>    | 0.34 <sup>+0.25</sup> <sub>-0.18</sub> | 45.0 <sup>+8.7</sup> <sub>-7.5</sub>    | 0.71 <sup>+0.11</sup> <sub>-0.11</sub> | 3400                         | 8.9 <sup>+0.4</sup> <sub>-0.6</sub>  |
| GW191204_171526  | 20.19 <sup>+1.64</sup> <sub>-0.95</sub> | 8.56 <sup>+0.41</sup> <sub>-0.28</sub> | 11.7 <sup>+3.3</sup> <sub>-1.7</sub>  | 8.4 <sup>+1.3</sup> <sub>-1.7</sub>    | 0.16 <sup>+0.08</sup> <sub>-0.05</sub>  | 0.64 <sup>+0.20</sup> <sub>-0.26</sub> | 0.13 <sup>+0.04</sup> <sub>-0.05</sub> | 19.18 <sup>+1.71</sup> <sub>-0.93</sub> | 0.73 <sup>+0.04</sup> <sub>-0.03</sub> | 310                          | 17.4 <sup>+0.2</sup> <sub>-0.3</sub> |
| GW191215_223052  | 43.3 <sup>+5.3</sup> <sub>-4.3</sub>    | 18.4 <sup>+2.2</sup> <sub>-1.7</sub>   | 24.9 <sup>+7.1</sup> <sub>-4.1</sub>  | 18.1 <sup>+3.8</sup> <sub>-4.1</sub>   | -0.04 <sup>+0.17</sup> <sub>-0.21</sub> | 1.93 <sup>+0.89</sup> <sub>-0.86</sub> | 0.35 <sup>+0.13</sup> <sub>-0.14</sub> | 41.4 <sup>+5.1</sup> <sub>-4.1</sub>    | 0.68 <sup>+0.07</sup> <sub>-0.07</sub> | 530                          | 11.2 <sup>+0.3</sup> <sub>-0.4</sub> |
| GW191216_213338  | 19.80 <sup>+2.70</sup> <sub>-0.93</sub> | 8.33 <sup>+0.22</sup> <sub>-0.19</sub> | 12.1 <sup>+4.6</sup> <sub>-2.2</sub>  | 7.7 <sup>+1.6</sup> <sub>-1.9</sub>    | 0.11 <sup>+0.13</sup> <sub>-0.06</sub>  | 0.34 <sup>+0.12</sup> <sub>-0.13</sub> | 0.07 <sup>+0.02</sup> <sub>-0.03</sub> | 18.87 <sup>+2.81</sup> <sub>-0.93</sub> | 0.70 <sup>+0.03</sup> <sub>-0.04</sub> | 910                          | 18.6 <sup>+0.2</sup> <sub>-0.2</sub> |
| GW191219_163120  | 32.3 <sup>+2.2</sup> <sub>-2.7</sub>    | 4.31 <sup>+0.12</sup> <sub>-0.17</sub> | 31.1 <sup>+2.2</sup> <sub>-2.8</sub>  | 1.17 <sup>+0.07</sup> <sub>-0.06</sub> | 0.00 <sup>+0.07</sup> <sub>-0.09</sub>  | 0.55 <sup>+0.24</sup> <sub>-0.16</sub> | 0.11 <sup>+0.05</sup> <sub>-0.03</sub> | 32.2 <sup>+2.2</sup> <sub>-2.7</sub>    | 0.14 <sup>+0.06</sup> <sub>-0.06</sub> | 1500                         | 9.1 <sup>+0.5</sup> <sub>-0.8</sub>  |
| GW191222_033537  | 79 <sup>+16</sup> <sub>-11</sub>        | 33.8 <sup>+7.1</sup> <sub>-5.0</sub>   | 45.1 <sup>+10.9</sup> <sub>-8.0</sub> | 34.7 <sup>+9.3</sup> <sub>-10.5</sub>  | -0.04 <sup>+0.20</sup> <sub>-0.25</sub> | 3.0 <sup>+1.7</sup> <sub>-1.7</sub>    | 0.51 <sup>+0.23</sup> <sub>-0.26</sub> | 75.5 <sup>+15.3</sup> <sub>-9.9</sub>   | 0.67 <sup>+0.08</sup> <sub>-0.11</sub> | 2000                         | 12.5 <sup>+0.2</sup> <sub>-0.3</sub> |
| GW191230_180458  | 86 <sup>+19</sup> <sub>-12</sub>        | 36.5 <sup>+8.2</sup> <sub>-5.6</sub>   | 49.4 <sup>+14.0</sup> <sub>-9.6</sub> | 37 <sup>+11</sup> <sub>-12</sub>       | -0.05 <sup>+0.26</sup> <sub>-0.31</sub> | 4.3 <sup>+2.1</sup> <sub>-1.9</sub>    | 0.69 <sup>+0.26</sup> <sub>-0.27</sub> | 82 <sup>+17</sup> <sub>-11</sub>        | 0.68 <sup>+0.11</sup> <sub>-0.13</sub> | 1100                         | 10.4 <sup>+0.3</sup> <sub>-0.4</sub> |
| GW200105_162426  | 11.0 <sup>+1.5</sup> <sub>-1.4</sub>    | 3.42 <sup>+0.08</sup> <sub>-0.08</sub> | 9.1 <sup>+1.7</sup> <sub>-1.7</sub>   | 1.91 <sup>+0.33</sup> <sub>-0.24</sub> | 0.17 <sup>+0.12</sup> <sub>-0.12</sub>  | 0.43 <sup>+0.12</sup> <sub>-0.12</sub> | 0.09 <sup>+0.02</sup> <sub>-0.02</sub> | 11.5 <sup>+1.5</sup> <sub>-1.5</sub>    | 0.95 <sup>+0.05</sup> <sub>-0.05</sub> | 6000                         | 11.0 <sup>+0.2</sup> <sub>-0.2</sub> |
| GW200112_155838  | 63.9 <sup>+5.7</sup> <sub>-4.6</sub>    | 27.4 <sup>+2.6</sup> <sub>-2.1</sub>   | 35.6 <sup>+6.7</sup> <sub>-4.5</sub>  | 28.3 <sup>+4.4</sup> <sub>-5.9</sub>   |   |  |  |   |  |                              |                                      |
| GW200115_042309  | 7.4 <sup>+1.7</sup> <sub>-1.7</sub>     | 2.43 <sup>+0.05</sup> <sub>-0.07</sub> | 5.9 <sup>+2.0</sup> <sub>-2.5</sub>   | 1.44 <sup>+0.85</sup> <sub>-0.28</sub> |   |  |  |   |  |                              |                                      |
| GW200128_022011  | 75 <sup>+17</sup> <sub>-12</sub>        | 32.0 <sup>+7.5</sup> <sub>-5.5</sub>   | 42.2 <sup>+11.6</sup> <sub>-8.1</sub> | 32.6 <sup>+9.5</sup> <sub>-9.2</sub>   |   |  |  |   |  |                              |                                      |
| GW200129_065458  | 63.3 <sup>+4.5</sup> <sub>-3.4</sub>    | 27.2 <sup>+2.1</sup> <sub>-2.3</sub>   | 34.5 <sup>+9.9</sup> <sub>-3.1</sub>  | 29.0 <sup>+3.3</sup> <sub>-9.3</sub>   |   |  |  |   |  |                              |                                      |
| GW200202_154313  | 17.58 <sup>+1.78</sup> <sub>-0.67</sub> | 7.49 <sup>+0.24</sup> <sub>-0.20</sub> | 10.1 <sup>+3.5</sup> <sub>-1.4</sub>  | 7.3 <sup>+1.1</sup> <sub>-1.7</sub>    |   |  |  |   |  |                              |                                      |
| GW200208_130117  | 65.3 <sup>+8.1</sup> <sub>-6.8</sub>    | 27.7 <sup>+3.7</sup> <sub>-3.1</sub>   | 37.7 <sup>+9.3</sup> <sub>-6.2</sub>  | 27.4 <sup>+6.3</sup> <sub>-7.3</sub>   |   |  |  |   |  |                              |                                      |
| GW200208_222617  | 63 <sup>+100</sup> <sub>-26</sub>       | 19.8 <sup>+10.5</sup> <sub>-5.2</sub>  | 51 <sup>+103</sup> <sub>-30</sub>     | 12.3 <sup>+9.2</sup> <sub>-5.5</sub>   |   |  |  |   |  |                              |                                      |
| GW200209_085452  | 62.6 <sup>+13.9</sup> <sub>-9.4</sub>   | 26.7 <sup>+6.0</sup> <sub>-4.2</sub>   | 35.6 <sup>+10.5</sup> <sub>-6.8</sub> | 27.1 <sup>+7.8</sup> <sub>-7.8</sub>   |   |  |  |   |  |                              |                                      |
| GW200210_092254  | 27.0 <sup>+7.1</sup> <sub>-4.3</sub>    | 6.56 <sup>+0.38</sup> <sub>-0.40</sub> | 24.1 <sup>+7.5</sup> <sub>-4.6</sub>  | 2.83 <sup>+0.47</sup> <sub>-0.42</sub> |   |  |  |   |  |                              |                                      |
| GW200216_220804  | 81 <sup>+20</sup> <sub>-14</sub>        | 32.9 <sup>+9.3</sup> <sub>-8.5</sub>   | 51 <sup>+22</sup> <sub>-13</sub>      | 30 <sup>+14</sup> <sub>-16</sub>       |   |  |  |   |  |                              |                                      |
| GW200219_094415  | 65.0 <sup>+12.6</sup> <sub>-8.2</sub>   | 27.6 <sup>+5.6</sup> <sub>-3.8</sub>   | 37.5 <sup>+10.1</sup> <sub>-6.9</sub> | 27.9 <sup>+7.4</sup> <sub>-8.4</sub>   |   |  |  |   |  |                              |                                      |
| GW200220_061928  | 148 <sup>+55</sup> <sub>-33</sub>       | 62 <sup>+23</sup> <sub>-15</sub>       | 87 <sup>+40</sup> <sub>-23</sub>      | 61 <sup>+26</sup> <sub>-25</sub>       |   |  |  |   |  |                              |                                      |
| GW200220_124850  | 67 <sup>+17</sup> <sub>-12</sub>        | 28.2 <sup>+7.3</sup> <sub>-5.1</sub>   | 38.9 <sup>+14.1</sup> <sub>-8.6</sub> | 27.9 <sup>+9.2</sup> <sub>-9.0</sub>   |   |  |  |   |  |                              |                                      |
| GW200224_222234  | 72.3 <sup>+7.2</sup> <sub>-5.3</sub>    | 31.1 <sup>+3.3</sup> <sub>-2.7</sub>   | 40.0 <sup>+6.7</sup> <sub>-4.5</sub>  | 32.7 <sup>+4.8</sup> <sub>-7.2</sub>   |   |  |  |   |  |                              |                                      |
| GW200225_060421  | 33.5 <sup>+3.6</sup> <sub>-3.0</sub>    | 14.2 <sup>+1.5</sup> <sub>-1.4</sub>   | 19.3 <sup>+5.0</sup> <sub>-3.0</sub>  | 14.0 <sup>+2.8</sup> <sub>-3.5</sub>   |   |  |  |   |  |                              |                                      |
| GW200302_015811  | 57.8 <sup>+9.6</sup> <sub>-6.9</sub>    | 23.4 <sup>+4.7</sup> <sub>-3.0</sub>   | 37.8 <sup>+8.7</sup> <sub>-8.5</sub>  | 20.0 <sup>+8.1</sup> <sub>-5.7</sub>   |   |  |  |   |  |                              |                                      |
| GW200306_093714  | 43.9 <sup>+11.8</sup> <sub>-7.5</sub>   | 17.5 <sup>+3.5</sup> <sub>-3.0</sub>   | 28.3 <sup>+17.1</sup> <sub>-7.7</sub> | 14.8 <sup>+6.5</sup> <sub>-6.4</sub>   |   |  |  |   |  |                              |                                      |
| GW200308_173609* | 92 <sup>+169</sup> <sub>-48</sub>       | 34 <sup>+44</sup> <sub>-18</sub>       | 60 <sup>+166</sup> <sub>-29</sub>     | 24 <sup>+36</sup> <sub>-13</sub>       |   |  |  |   |  |                              |                                      |
| GW200311_115853  | 61.9 <sup>+5.3</sup> <sub>-4.2</sub>    | 26.6 <sup>+2.4</sup> <sub>-2.0</sub>   | 34.2 <sup>+6.4</sup> <sub>-3.8</sub>  | 27.7 <sup>+4.1</sup> <sub>-5.9</sub>   |   |  |  |   |  |                              |                                      |
| GW200316_215756  | 21.2 <sup>+7.2</sup> <sub>-2.0</sub>    | 8.75 <sup>+0.62</sup> <sub>-0.55</sub> | 13.1 <sup>+10.2</sup> <sub>-2.9</sub> | 7.8 <sup>+2.0</sup> <sub>-2.9</sub>    |   |  |  |   |  |                              |                                      |
| GW200322_091133* | 50 <sup>+132</sup> <sub>-22</sub>       | 15.0 <sup>+29.5</sup> <sub>-4.0</sub>  | 38 <sup>+130</sup> <sub>-22</sub>     | 11.3 <sup>+24.3</sup> <sub>-6.0</sub>  |   |  |  |   |  |                              |                                      |



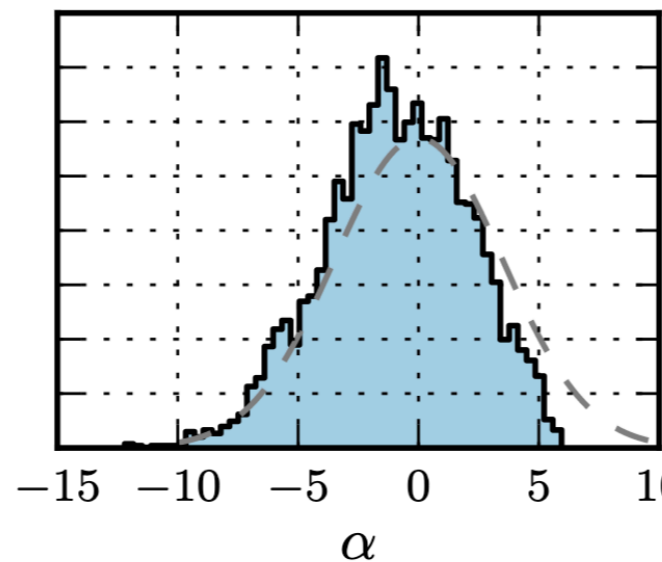
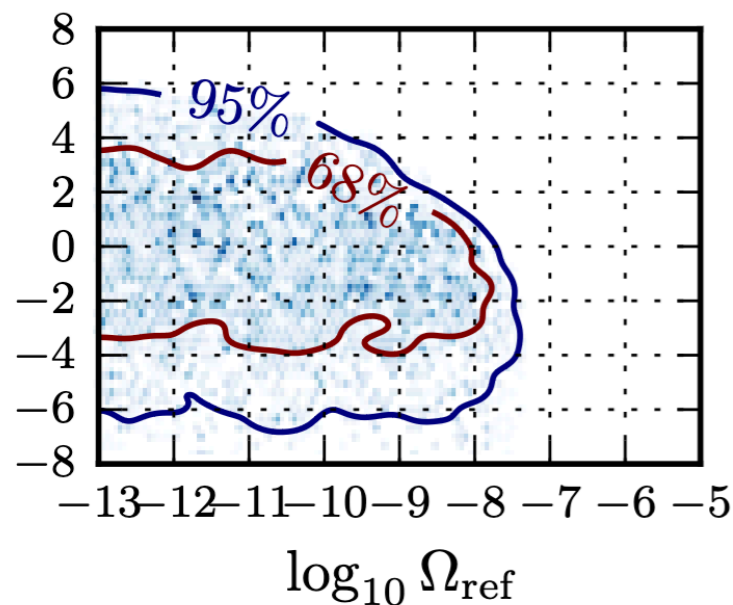
# Earth-based interferometers

Stochastic GW background: for now, only upper bounds

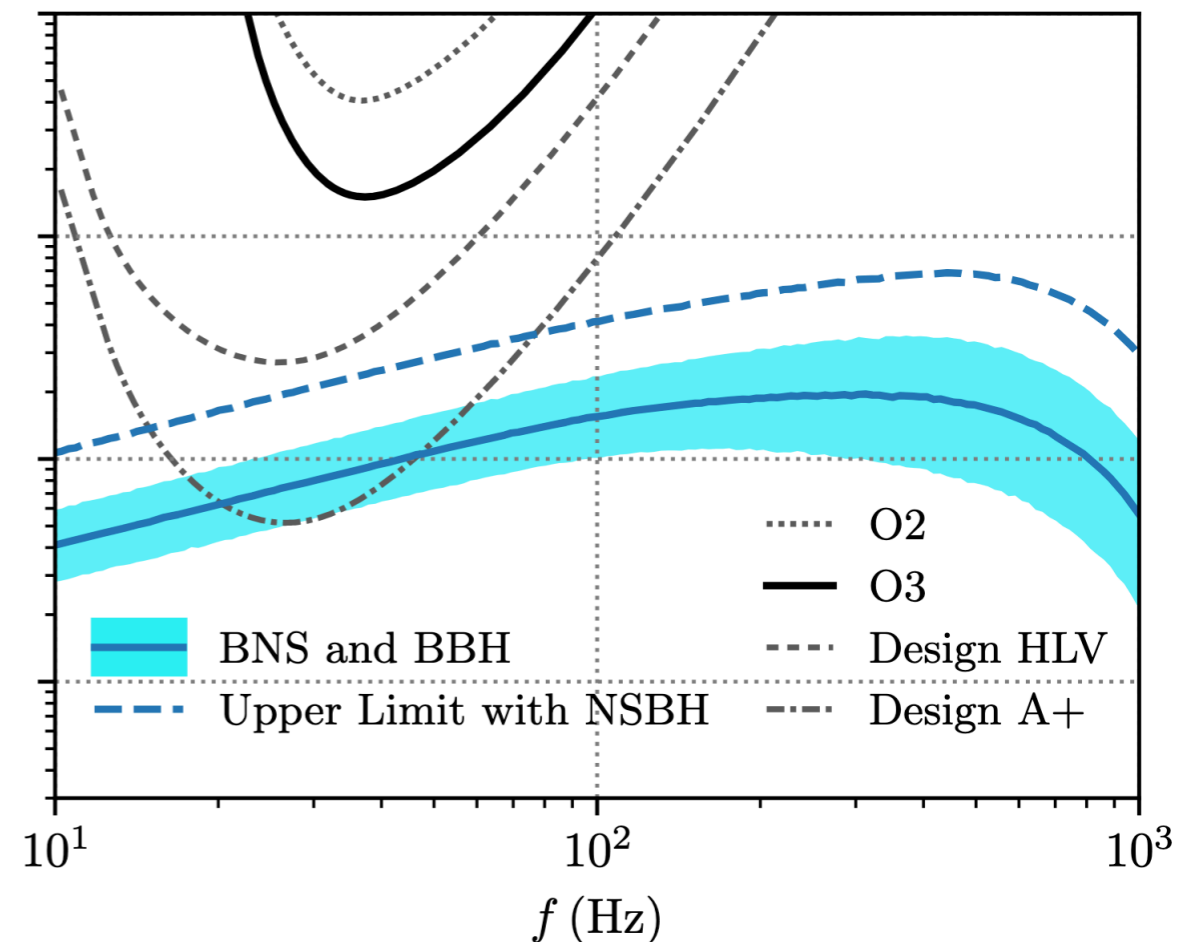


Upper bound on generic

$$\Omega_{\text{GW}}(f) = \Omega_{\text{ref}} \left( \frac{f}{25 \text{ Hz}} \right)^\alpha$$



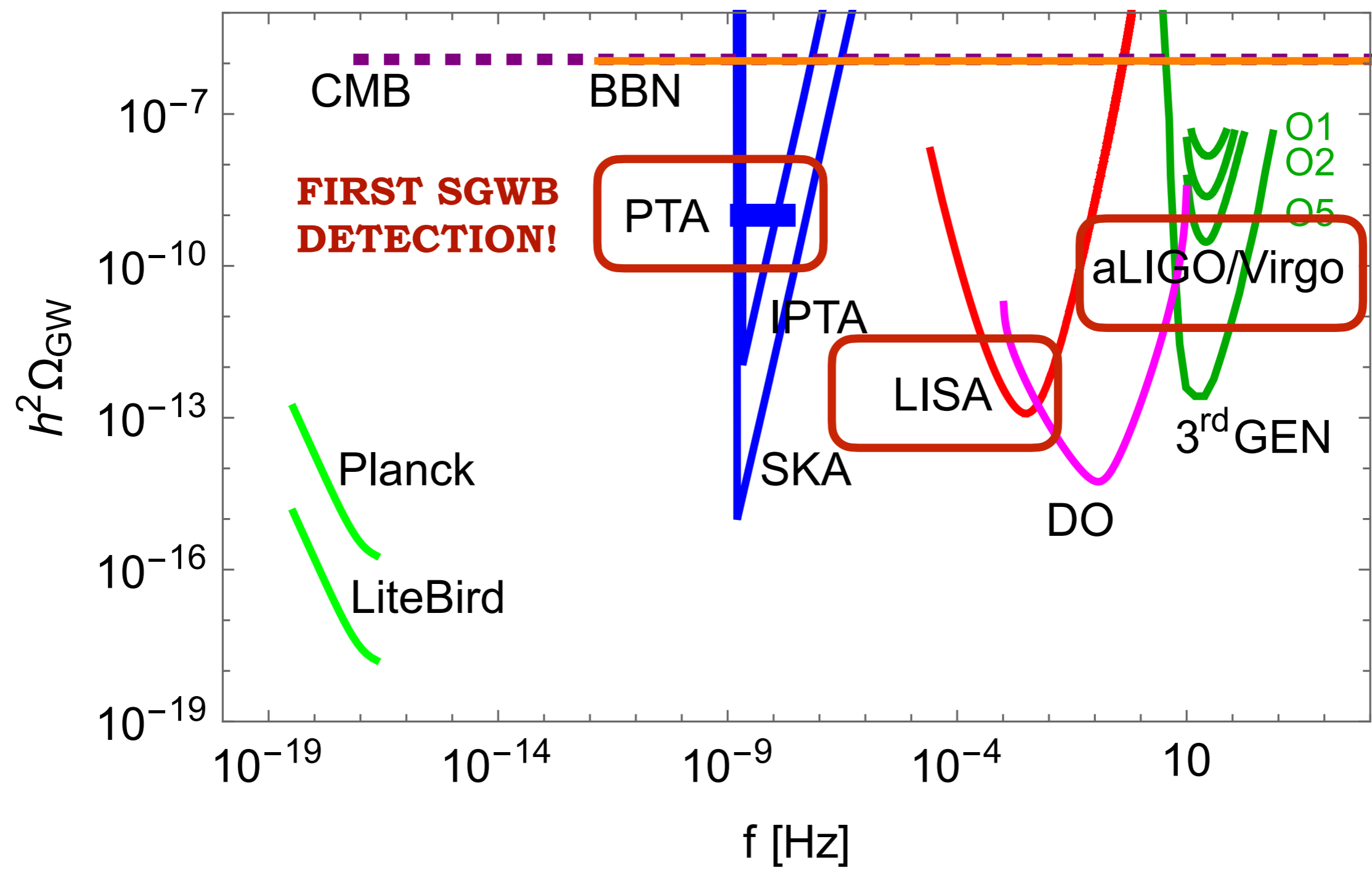
SGWB from BHBs and NSBs



Detection via cross-correlation of signals from different detectors

# What is/will be known about the SGWB

## Present and future GW detection facilities





# Space-based interferometers: LISA

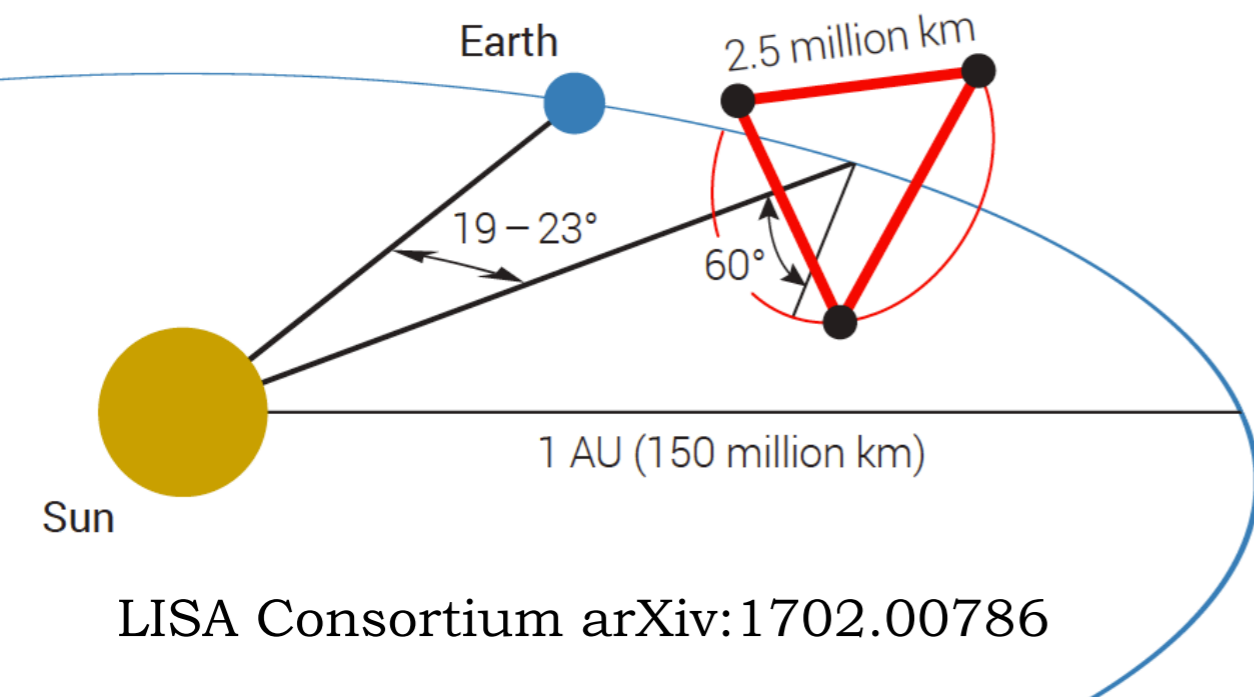
## LISA: Laser Interferometer Space Antenna

- no seismic noise
- much longer arms than on Earth

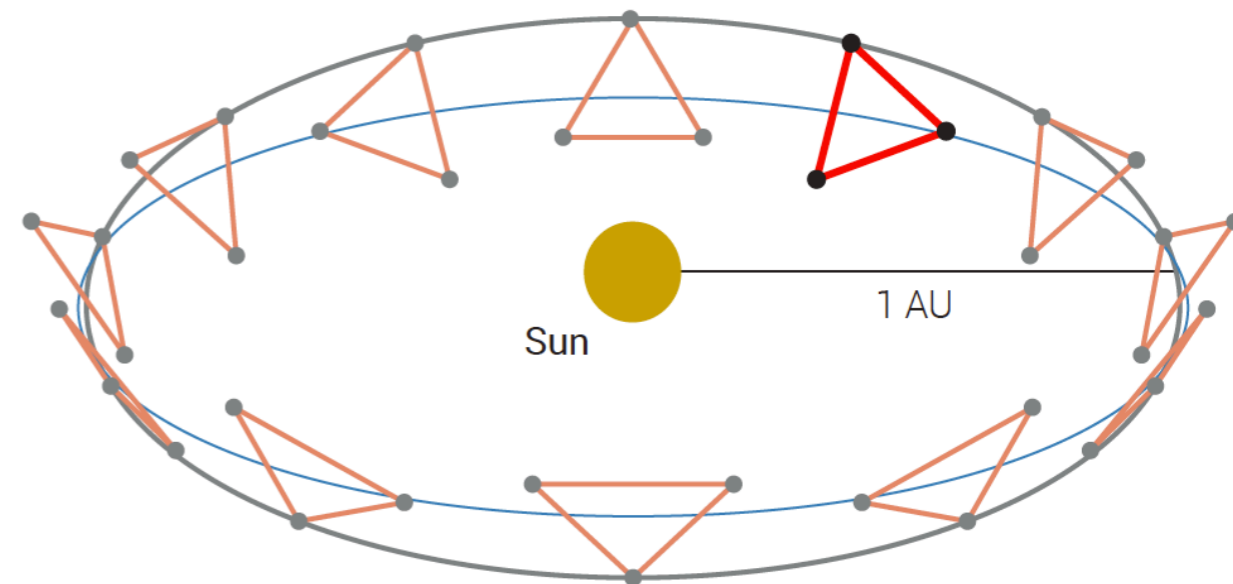
frequency range of detection:

$$10^{-4} \text{ Hz} < f < 1 \text{ Hz}$$

- Launch in ~2034
- two masses in free fall per spacecraft
- 2.5 million km arms
- picometer displacement of masses

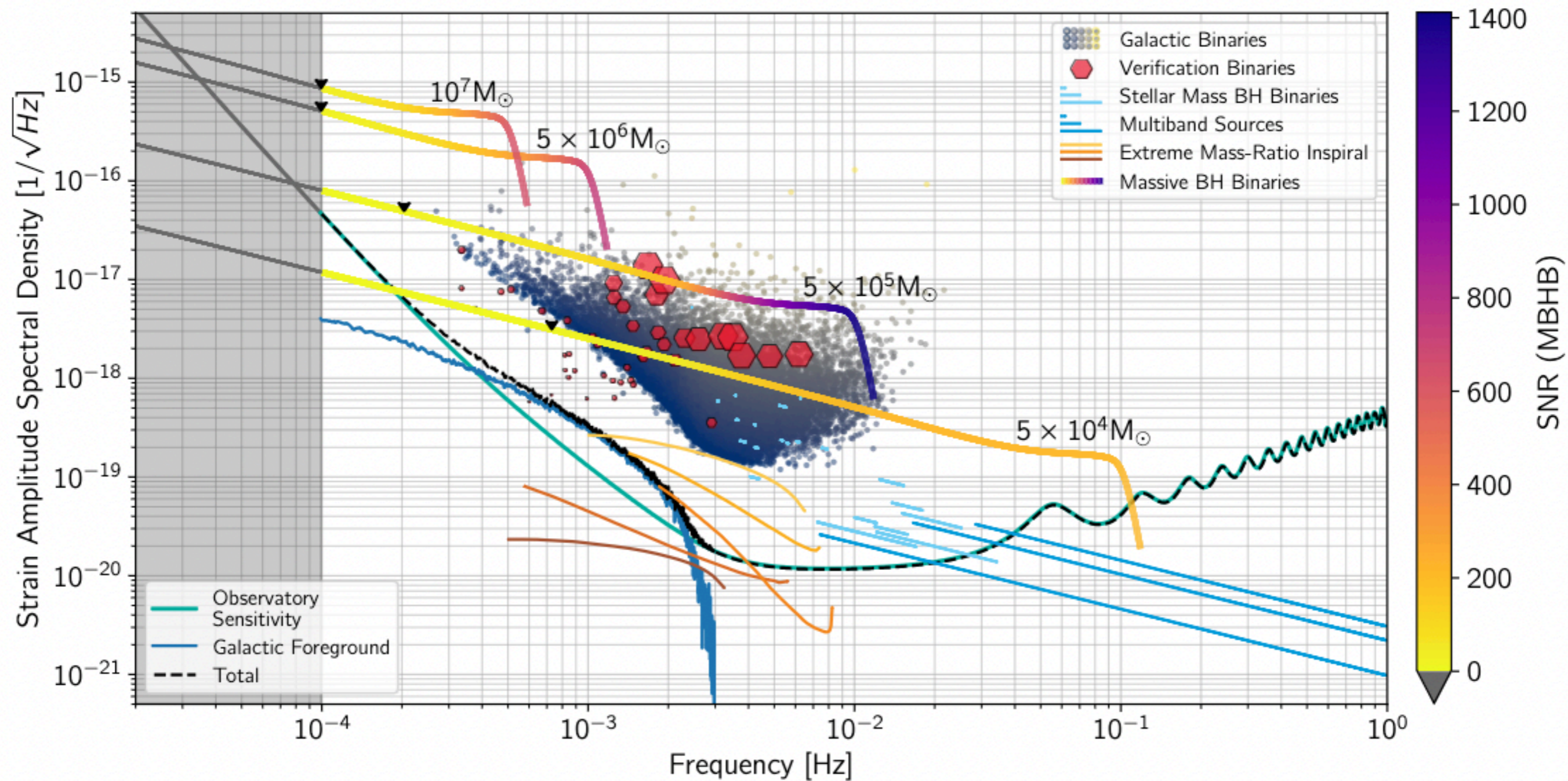


LISA Consortium arXiv:1702.00786



# Space-based interferometers: LISA

## DETECTION TARGETS:

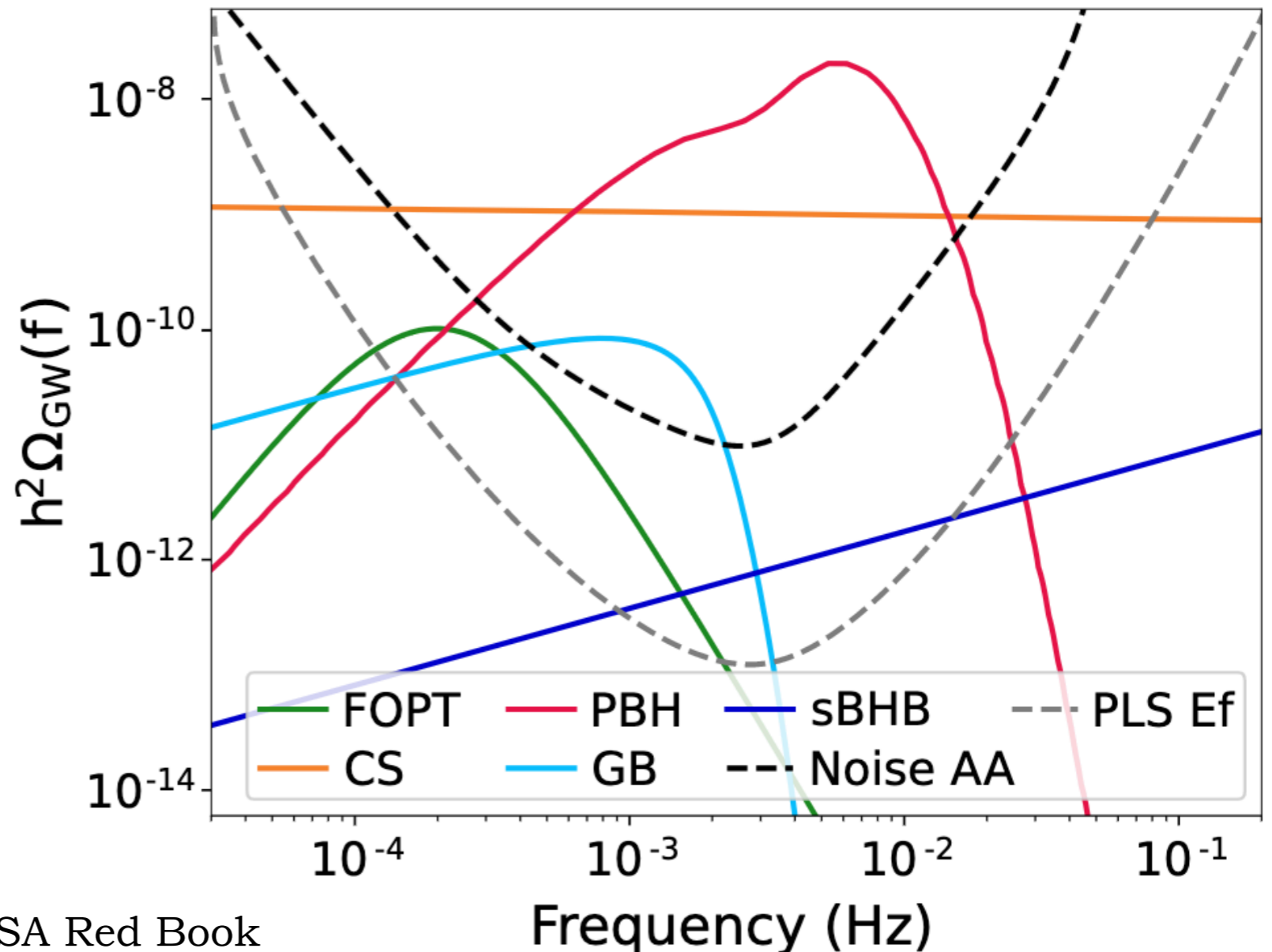


# Space-based interferometers: LISA

## Stochastic GW background

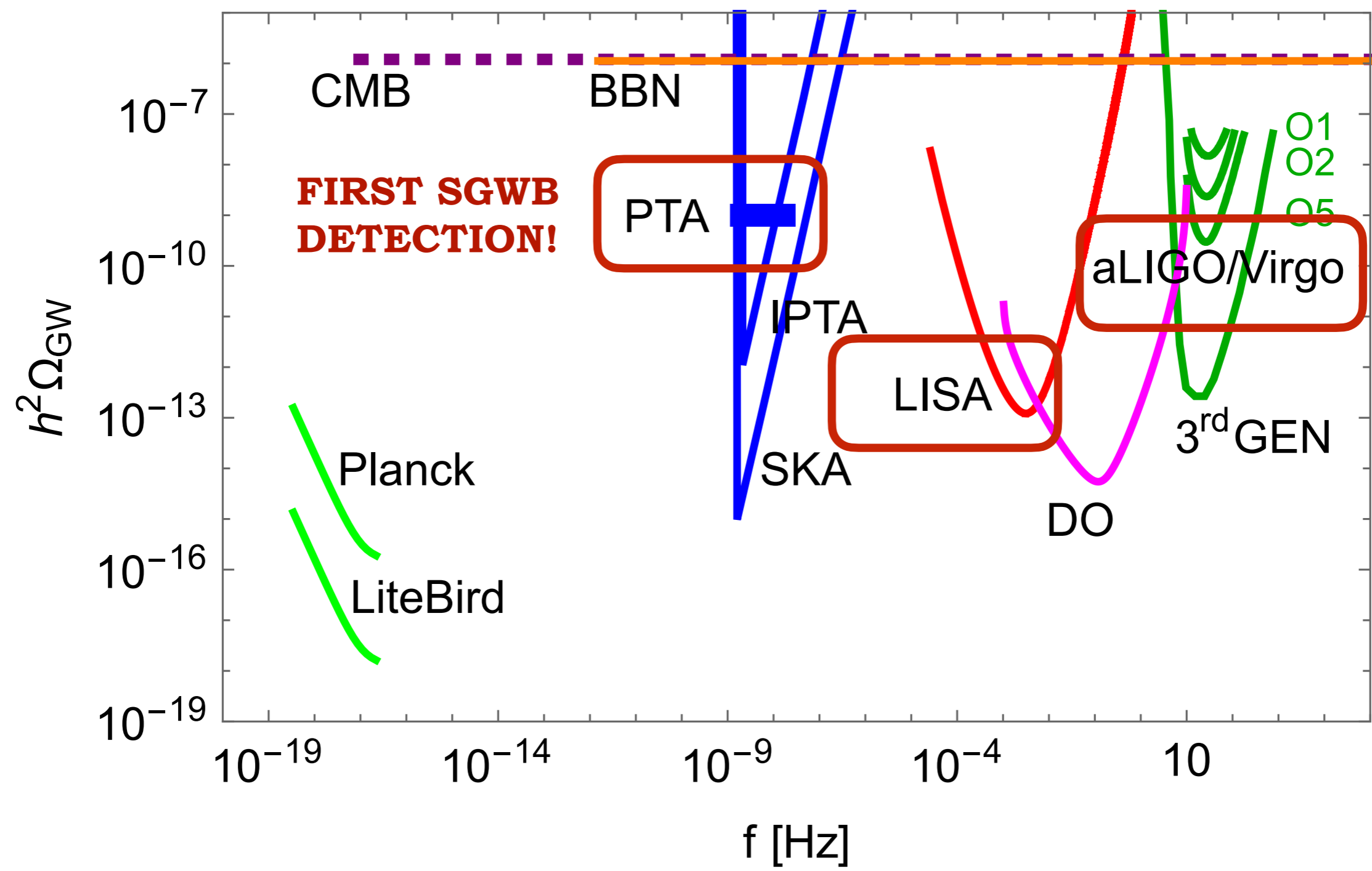
- Confusion noise from the binaries in the Galaxy (mainly WD binaries)
- Confusion noise from extra-galactic binaries (WD binaries and BHBs)
- Candidates from the early universe, in particular at the EW scale

Detecting a SGWB with LISA is challenging: no cross-correlation, need to assume knowledge of the noise (possibility of null channels)



# What is/will be known about the SGWB

## Present and future GW detection facilities





# Pulsar timing arrays

CPTA, EPTA, NANOGrav, PPTA -> IPTA

frequency range of detection:  $10^{-9} \text{ Hz} < f < 10^{-7} \text{ Hz}$

- rotating, magnetised neutron stars emitting periodic radio-frequency EM pulses -> can be used as clocks in the sky
- the radio pulses are emitted at very regular time intervals, but their arrival times can be altered by a GW passing between the pulsar and the Earth
- First a timing model of the pulsar is constructed, which is then compared to observations to infer the *timing residuals* where the GW effect is looked for

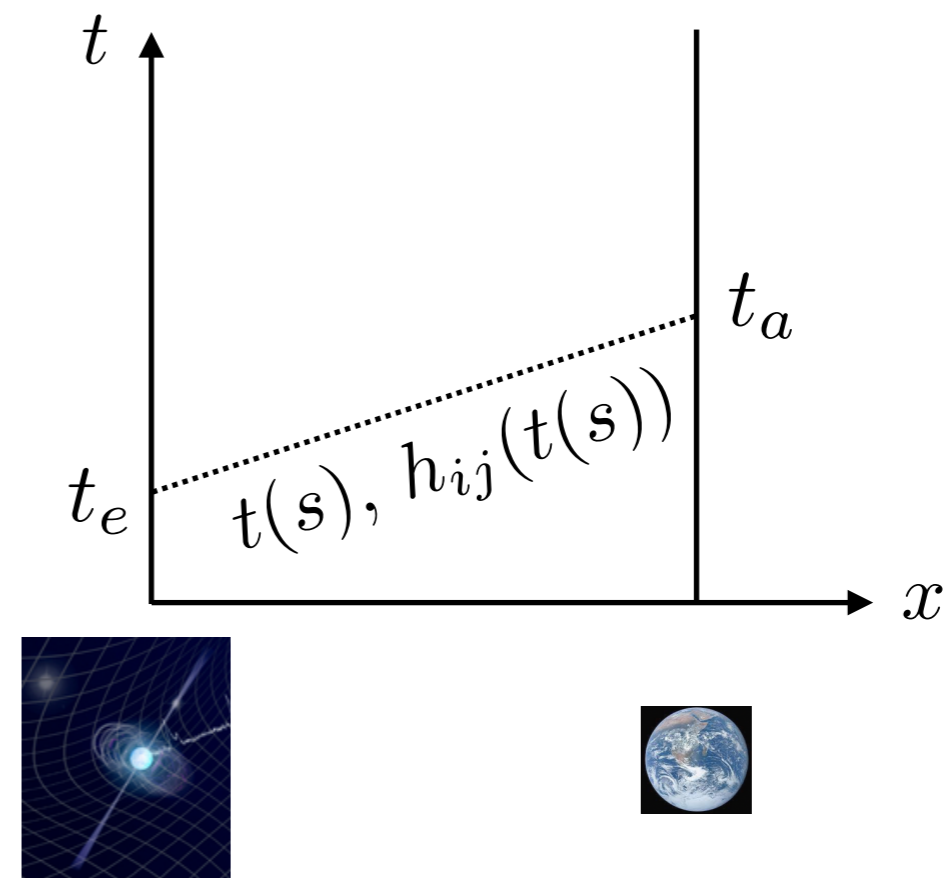
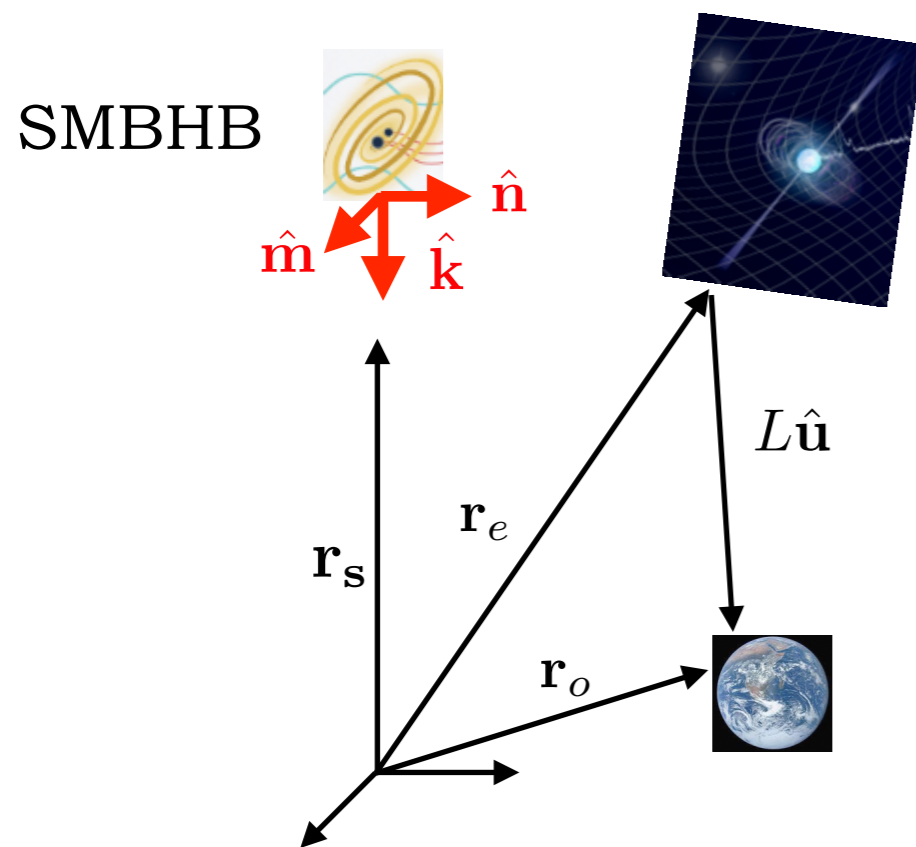


## DETECTION TARGETS:

Individual emission and stochastic background from inspiralling Super Massive Black Hole Binaries (SMBHBs) with masses  $\sim 10^9 M_{\odot}$  at the centre of galaxies

# Pulsar timing arrays

**Principle of the measurement:** gravitational redshift caused by gravitational waves emitted by far-away sources and travelling through spacetime between the pulsars and the Earth



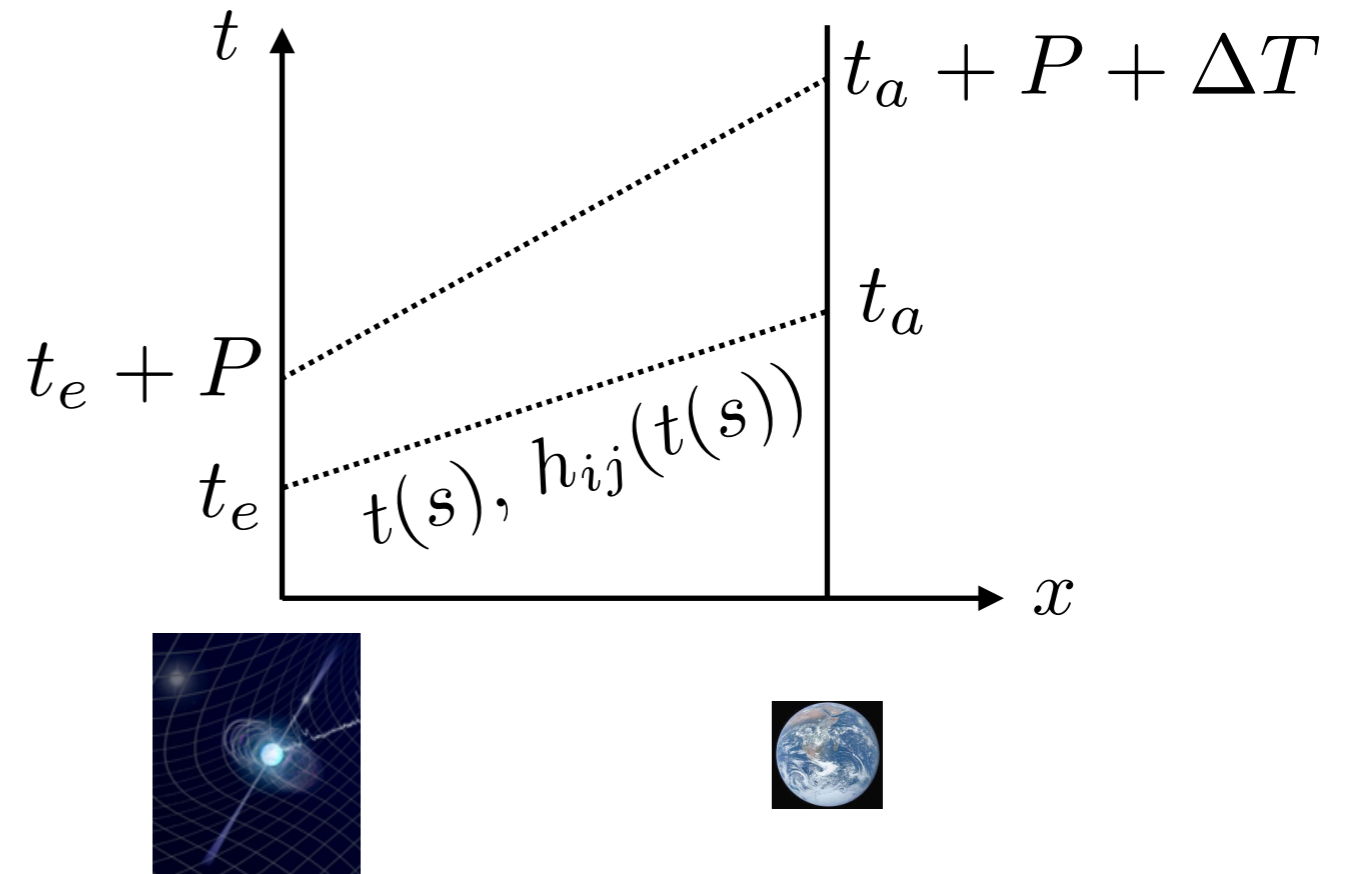
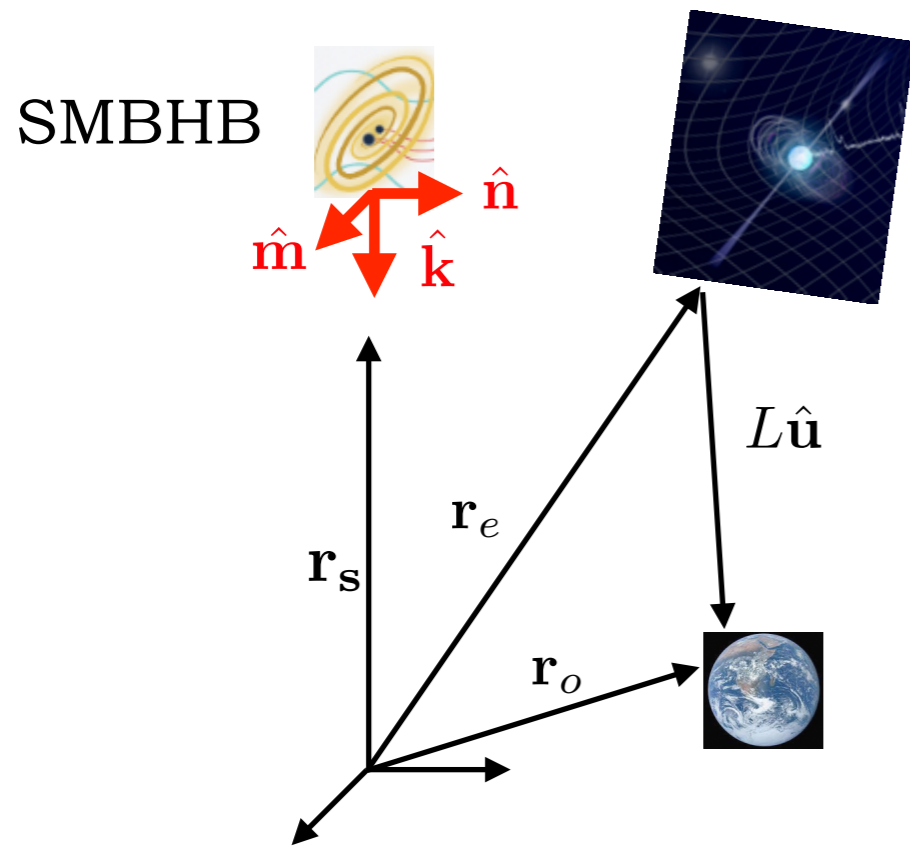
Photon from pulsar:

$$dt = \pm \sqrt{(\delta_{ij} + h_{ij}) dx^i dx^j} \quad t_a - t_e = L + \frac{1}{2} \hat{u}^i \hat{u}^j \int_0^L ds h_{ij}(t_e + s, \mathbf{r}_e + s \hat{\mathbf{u}})$$

Effect of the metric perturbation on a single beam:  
not measurable unless one knows the reference quantities

# Pulsar timing arrays

Principle of the measurement: compare with the next pulse

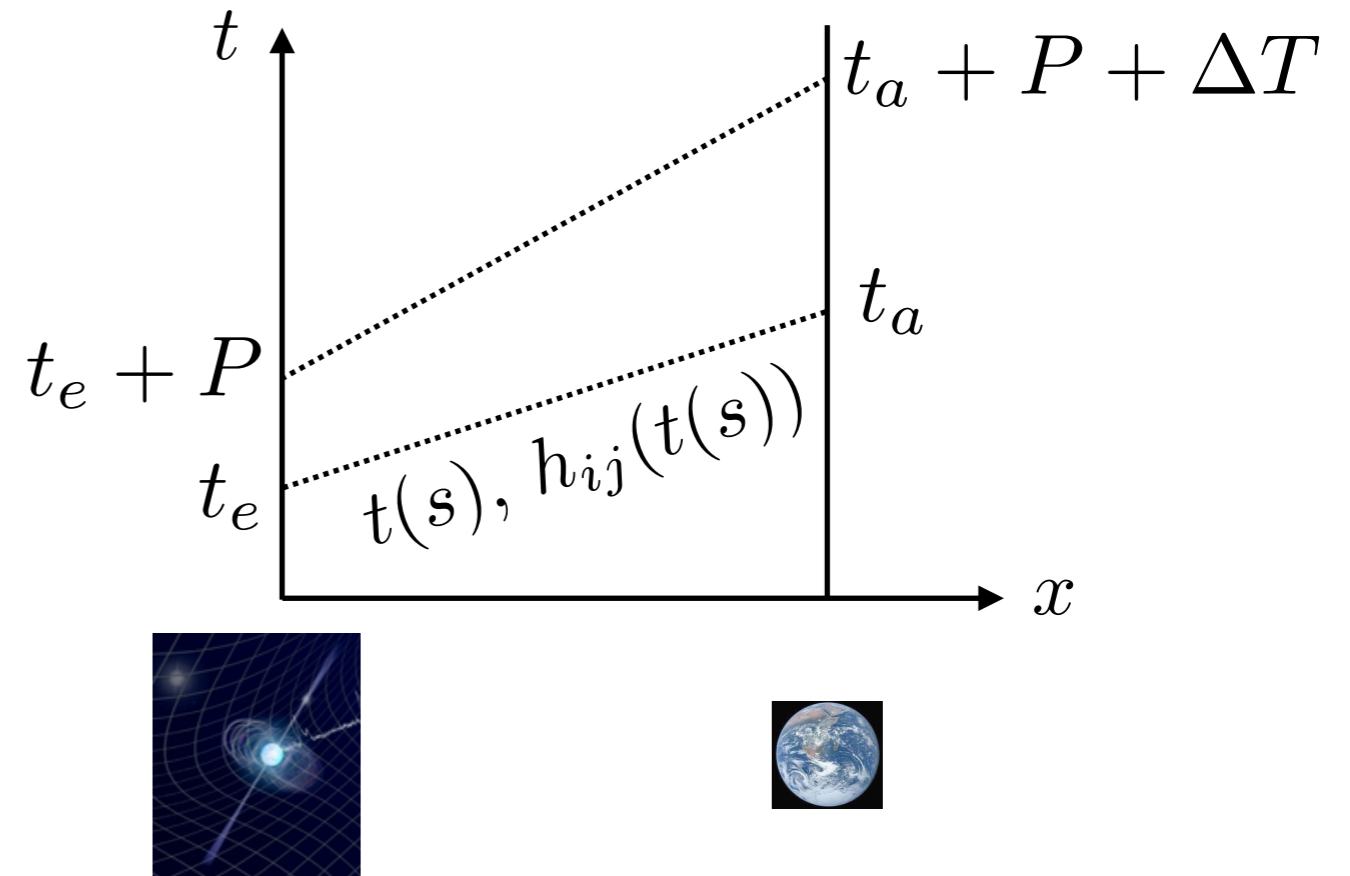
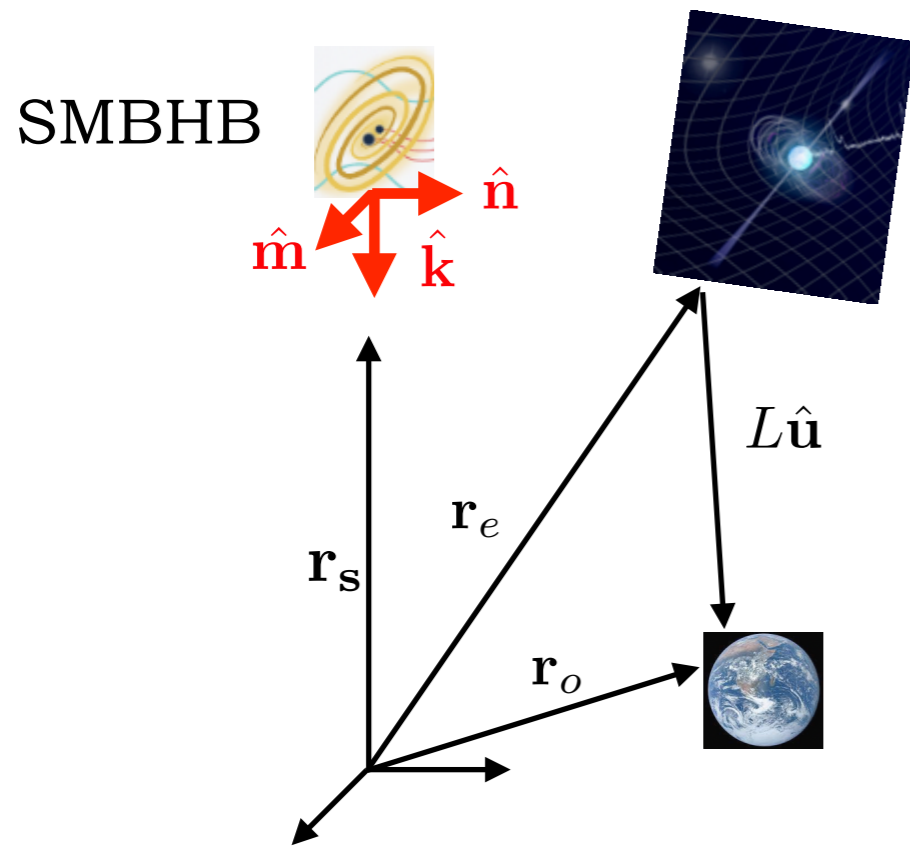


$$\Delta T = \frac{1}{2} \hat{u}^i \hat{u}^j \int_0^L ds [h_{ij}(t_e + P + s, \mathbf{r}_e + s\hat{\mathbf{u}}) - h_{ij}(t_e + s, \mathbf{r}_e + s\hat{\mathbf{u}})]$$

This effect is present only because the gravitational wave is **time-dependent**

# Pulsar timing arrays

Principle of the measurement: compare with the next pulse



$$\Delta T = \frac{1}{2} \frac{\hat{u}^i \hat{u}^j}{1 - \hat{\mathbf{k}} \cdot \hat{\mathbf{u}}} \int_{t_e - \hat{\mathbf{k}} \cdot \mathbf{r}_e}^{t_e + L - \hat{\mathbf{k}} \cdot \mathbf{r}_e - L \hat{\mathbf{k}} \cdot \mathbf{u}} dX [h_{ij}(X + P) - h_{ij}(X)]$$

Wave propagating in  $\mathbf{k}$  direction:  $h_{ij}(X)$  with  $X = t_e + s - \hat{\mathbf{k}} \cdot \mathbf{r}_e - s \hat{\mathbf{k}} \cdot \hat{\mathbf{u}}$



# Pulsar timing arrays

Supposing the source is the inspiral of a super massive black hole binary:  
 what is the typical scale of the time variation of the metric perturbation?

$$f(\tau) = \frac{1}{\pi} \left( \frac{5}{256} \right)^{3/8} \frac{1}{(G M_c)^{5/8} \tau^{3/8}} \simeq 10^{-8} \text{ Hz} \quad \text{for} \quad \begin{array}{l} M_c \simeq 10^9 M_\odot \\ \tau = 4 \times 10^4 \text{ yrs} \\ \text{Time to coalescence} \end{array}$$

Chirp mass

$$M_c = \frac{(m_1 m_2)^{3/5}}{(m_1 + m_2)^{1/5}}$$

GW varies on  
 a scale of  
 about 3 years

Period of the  
 pulsar:  
 millisecond

$$f_{\text{GW}} P \ll 1$$

$$\Delta T = \frac{1}{2} \frac{\hat{u}^i \hat{u}^j}{1 - \hat{\mathbf{k}} \cdot \hat{\mathbf{u}}} \int_{t_e - \hat{\mathbf{k}} \cdot \mathbf{r}_e}^{t_e + L - \hat{\mathbf{k}} \cdot \mathbf{r}_e - L \hat{\mathbf{k}} \cdot \mathbf{u}} dX [h_{ij}(X + P) - h_{ij}(X)] \quad \text{Taylor expand}$$

Relative change  
 in the rate of the  
 pulses measured on  
 Earth because of the  
 GW passing by:

$$\frac{\Delta T}{P} \simeq \frac{1}{2} \frac{\hat{u}^i \hat{u}^j}{1 - \hat{\mathbf{k}} \cdot \hat{\mathbf{u}}} [h_{ij}(t_e + L, \mathbf{r}_o) - h_{ij}(t_e, \mathbf{r}_e)]$$

Earth term                      Pulsar term

# Pulsar timing arrays

Supposing the source is the inspiral of a super massive black hole binary:  
 what is the typical scale of the time variation of the metric perturbation?

$$f(\tau) = \frac{1}{\pi} \left( \frac{5}{256} \right)^{3/8} \frac{1}{(G M_c)^{5/8} \tau^{3/8}} \simeq 10^{-8} \text{ Hz} \quad \text{for} \quad \begin{array}{l} M_c \simeq 10^9 M_\odot \\ \tau = 4 \times 10^4 \text{ yrs} \\ \text{Time to coalescence} \end{array}$$

Chirp mass

$$M_c = \frac{(m_1 m_2)^{3/5}}{(m_1 + m_2)^{1/5}}$$

GW varies on  
 a scale of  
 about 3 years

Period of the  
 pulsar:  
 millisecond

$$f_{\text{GW}} P \ll 1$$

$$\Delta T = \frac{1}{2} \frac{\hat{u}^i \hat{u}^j}{1 - \hat{\mathbf{k}} \cdot \hat{\mathbf{u}}} \int_{t_e - \hat{\mathbf{k}} \cdot \mathbf{r}_e}^{t_e + L - \hat{\mathbf{k}} \cdot \mathbf{r}_e - L \hat{\mathbf{k}} \cdot \mathbf{u}} dX [h_{ij}(X + P) - h_{ij}(X)] \quad \text{Taylor expand}$$

NB: this is the change in the frequency of the pulses due to the GWs, calculated between two successive geodesics, and NOT the redshift experienced by a photon on the same geodesic (usual gravitational redshift, depending on  $\dot{h}_{ij}$ )

However, the two expressions become the same in the limit of infinitesimal P

# Pulsar timing arrays

Relative change  
in the rate of the  
pulses measured on  
Earth because of  
the GW passing by:

$$\frac{\Delta T}{P} \simeq \frac{1}{2} \frac{\hat{u}^i \hat{u}^j}{1 - \hat{\mathbf{k}} \cdot \hat{\mathbf{u}}} [h_{ij}(t_e + L, \mathbf{r}_o) - h_{ij}(t_e, \mathbf{r}_e)]$$

$$\sim 7 \cdot 10^{-23} \frac{\text{pc}}{d_L} \left( \frac{M_c}{M_\odot} \right)^{5/3} \left( \frac{f_{\text{GW}}}{10^{-8} \text{ Hz}} \right)^{2/3} \simeq 7 \cdot 10^{-16}$$

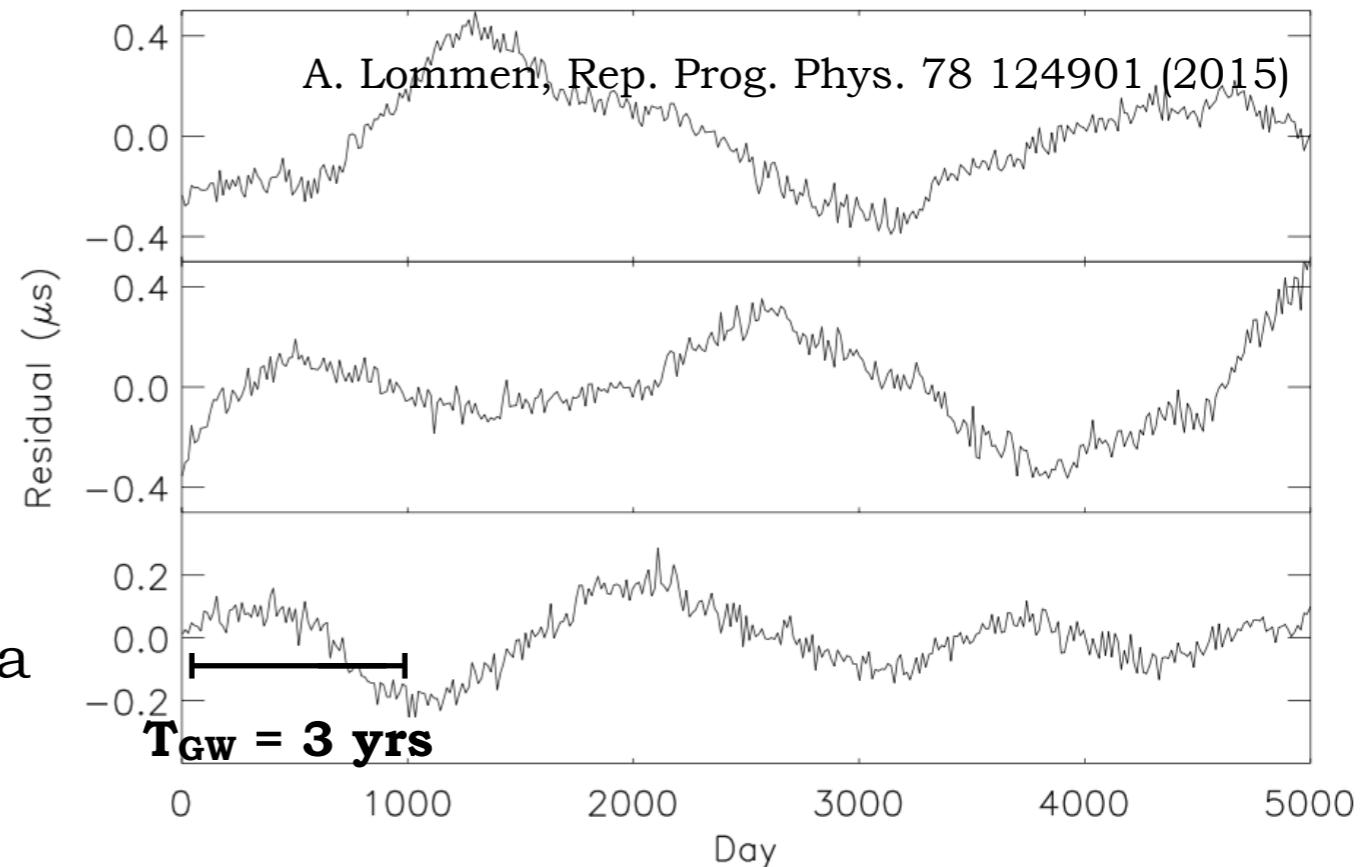
↑  
 $M_c \simeq 10^9 M_\odot$   
 $d_L = 100 \text{ Mpc}$

Timing residuals:  $R(T) = \int_{t_{\text{ref}}}^{t_{\text{ref}}+T} dt \frac{\Delta T}{P}$

$$R(T_{\text{GW}} = 3 \text{ yrs}) \simeq 60 \text{ nsec}$$

A GW with period of a few years induces a timing residual of order 100 nsec, the precision of pulsar monitoring!

This renders the measurement possible, provided one has at least a few years of data

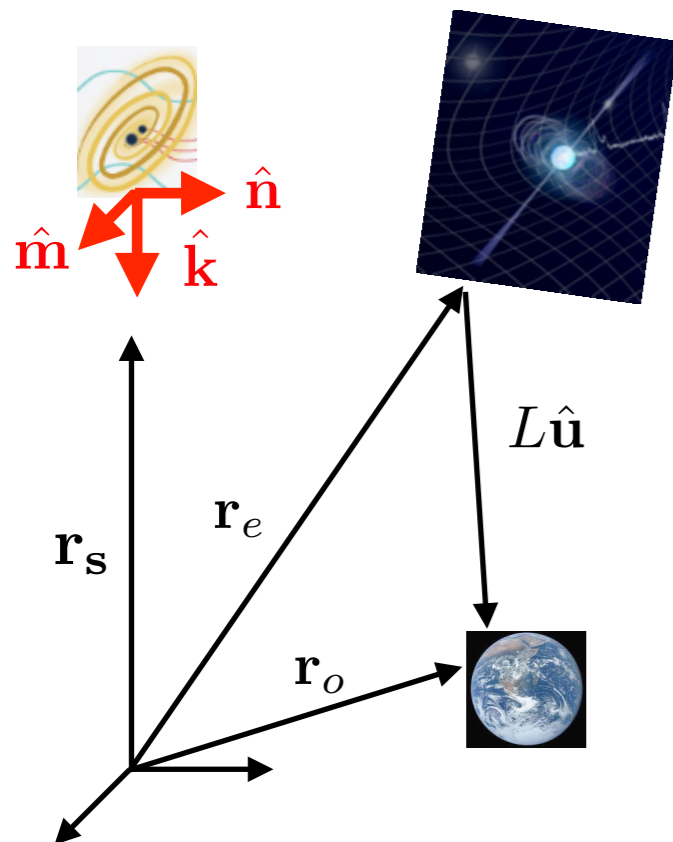


# Pulsar timing arrays

HOWEVER! The signal from a single pulsar is very noisy: varying morphology of the pulses, propagation noise due to the dispersion by the interstellar medium, time referencing (time standards and solar system barycentre)...

## Correlation between many pulsars to beat down the noise

$$\frac{\Delta T}{P} \simeq \frac{1}{2} \frac{\hat{u}^i \hat{u}^j}{1 - \hat{\mathbf{k}} \cdot \hat{\mathbf{u}}} [h_{ij}(t_e + L, \mathbf{r}_o) - h_{ij}(t_e, \mathbf{r}_e)]$$



Earth term:

GW left the source at  
time

$$t_e + L - |\mathbf{r}_o - \mathbf{r}_s|$$

Pulsar term:

GW left the source at  
time

$$t_e - |\mathbf{r}_e - \mathbf{r}_s|$$

This term is different for  
each pulsar

In the correlation the Earth term in general dominates,  
but the pulsar term can create noise (unless one can  
determine the delay of each pulsar)

# Pulsar timing arrays

## Response of a pair of pulsars to a stochastic GW background

$$\langle R_a(T) R_b(T) \rangle = \int_{t_{\text{ref}}}^{t_{\text{ref}}+T} dt' \int_{t_{\text{ref}}}^{t_{\text{ref}}+T} dt'' \left\langle \frac{\Delta T}{P}(t') \Big|_a \frac{\Delta T}{P}(t'') \Big|_b \right\rangle$$

$$\frac{\Delta T}{P}(t') \Big|_a = \sum_r \int \frac{d\mathbf{k}^3}{(2\pi)^3} h_r(\mathbf{k}) F_a^r(\hat{\mathbf{k}}) e^{-ik(t' - \hat{\mathbf{k}} \cdot \mathbf{r}_o)} \left[ 1 - e^{ikL_a(1 - \hat{\mathbf{k}} \cdot \hat{\mathbf{u}}_a)} \right]$$

“Detector response”  $F_a^r(\hat{\mathbf{k}}) = \frac{\hat{u}_a^i \hat{u}_a^j e_{ij}^r(\hat{\mathbf{k}})}{2(1 - \hat{\mathbf{k}} \cdot \hat{\mathbf{u}})}$

put Earth at origin to simplify

Earth term

Pulsar term

Use SGWB power spectrum

$$\langle h_r(\mathbf{k}, \eta) h_p^*(\mathbf{q}, \eta) \rangle = \frac{8\pi^5}{k^3} \delta^{(3)}(\mathbf{k} - \mathbf{q}) \delta_{rp} h_c^2(k, \eta)$$

The Earth term dominates

$$\left[ 1 - e^{ikL_a(1 - \hat{\mathbf{k}} \cdot \hat{\mathbf{u}}_a)} \right] \left[ 1 - e^{-ikL_b(1 - \hat{\mathbf{k}} \cdot \hat{\mathbf{u}}_b)} \right] \simeq 1$$

$$kL_a = \mathcal{O}(2\pi \cdot 10^{-8} \text{ Hz} \cdot 500 \text{ pc}) = \mathcal{O}(3000) \gg 1$$

$a \neq b$   
and SMBHB not in pulsar direction

# Pulsar timing arrays

## Response of a pair of pulsars to a stochastic GW background

$$\langle R_a(T) R_b(T) \rangle = \int_{t_{\text{ref}}}^{t_{\text{ref}}+T} dt' \int_{t_{\text{ref}}}^{t_{\text{ref}}+T} dt'' \left\langle \frac{\Delta T}{P}(t') \Big|_a \frac{\Delta T}{P}(t'') \Big|_b \right\rangle$$

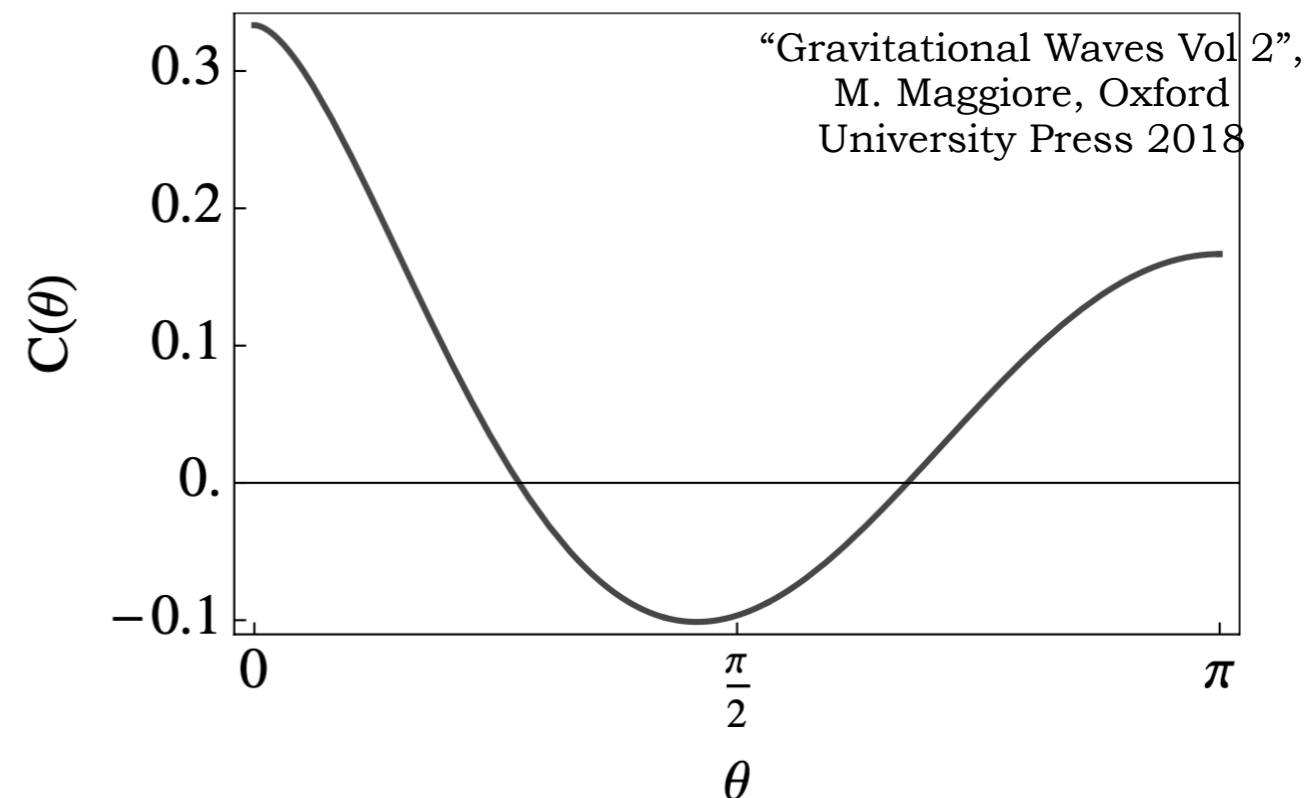
$\theta_{ab}$  angle between pulsars

$$= \mathcal{C}(\theta_{ab}) \int_0^\infty df \frac{h_c^2(f)}{(2\pi)^2 f^3} [1 + \cos(2\pi f(T - t_{\text{ref}}))]$$

*Hellings and Downs curve*, characteristic of a GW signal because consequence of the quadrupolar nature of GWs

$$\begin{aligned} \mathcal{C}(\theta_{ab}) &= \int \frac{d\hat{\mathbf{k}}}{4\pi} \sum_r F_r^a(\hat{\mathbf{k}}) F_r^b(\hat{\mathbf{k}}) \\ &= \frac{1}{3} - \frac{1}{6} x_{ab} + x_{ab} \log(x_{ab}) \end{aligned}$$

$$x_{ab} = \frac{1}{2} (1 - \cos \theta_{ab})$$





# Pulsar timing arrays

Observation of the *Hellings and Downs curve* is **smoking gun evidence** of GW detection

(not only SGWB but also from a single SMBHB - Cornish & Sesana arXiv:1305.0326)

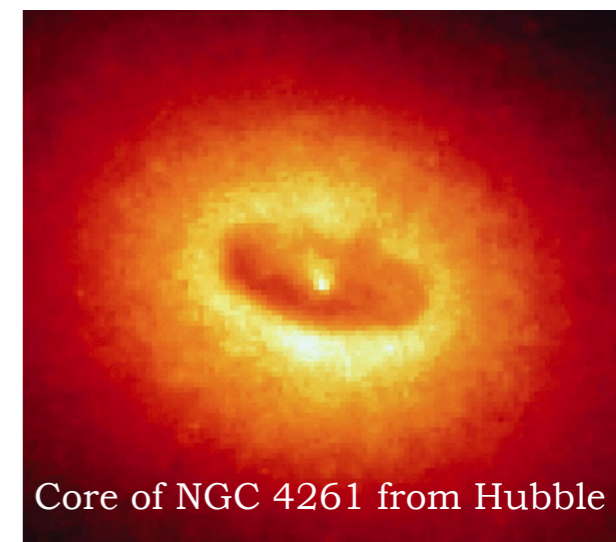
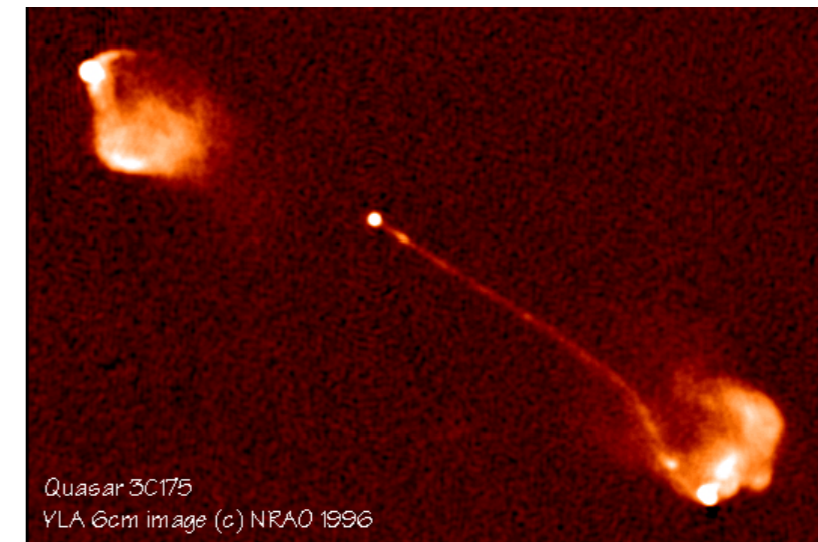
time referencing errors generate a correlated noise but:

- noise from uncertainties on the time standards on Earth is independent on the pulsar angles
- noise from uncertainties on the solar system barycentre position take the form of a (rotating) dipole (dependent on the cosine of the angle) -> can contaminate the quadrupole

A SGWB from SMBHBs is the best candidate source in PTA frequency band

## What are SMBHBs?

- They have been observed in the core of galaxies and are the central engine of active galactic nuclei
- They can originate from the collapse of massive stars ( $\sim 100 M_{\odot}$ ) or gas clouds ( $\sim 10^4 M_{\odot}$ ), and then grow in mass through gas accretion and/or mergers following the collision of their host galaxies (but their origin is still to be confirmed, they can also be primordial...)
- JWST sees SMBHBs up to very high redshift  $z \sim 11$
- Their presence is linked to the formation of galaxies and matter structure in the Universe



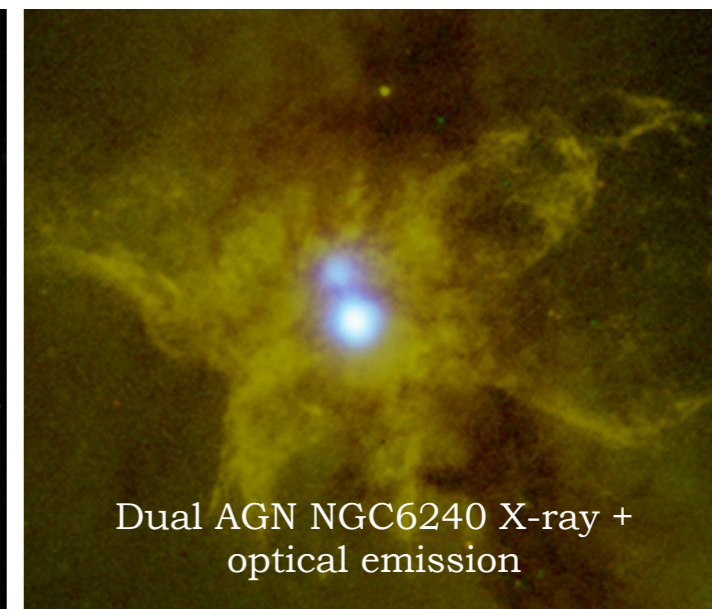
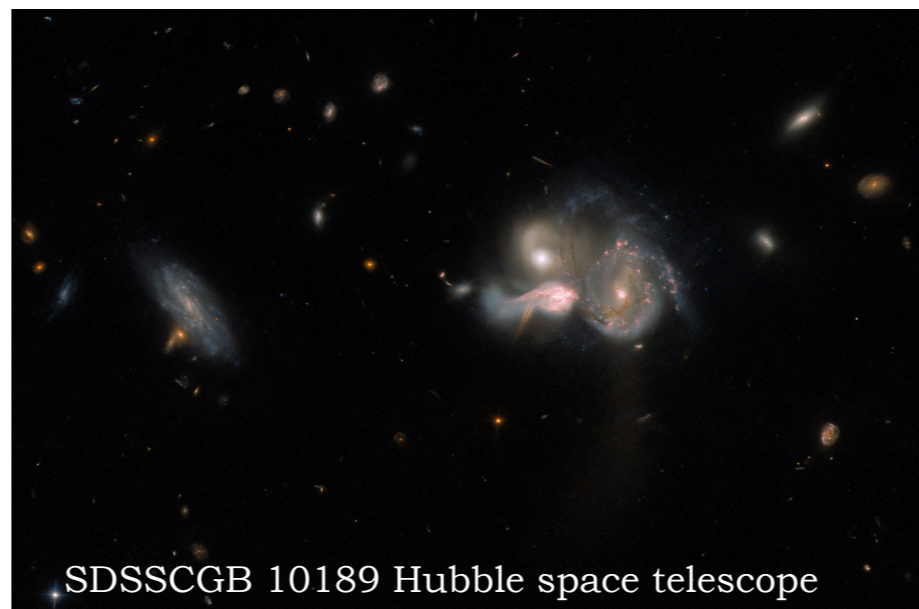
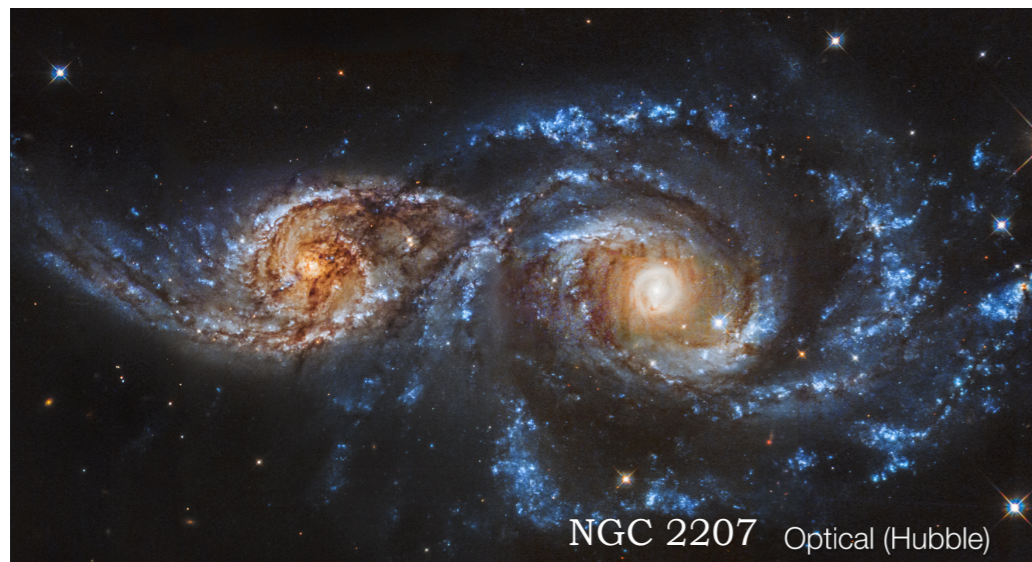


# Pulsar timing arrays

## HOWEVER!

- To emit GWs, SMBHs must be paired in gravitationally bound binaries in the GW emitting regime: separation of  $\sim 0.01$ - $0.001$  pc
- Binaries can be formed after the collision of two galaxies: the MBH previously at the centre of galaxies get to  $\sim$  kpc separation (X-ray evidence from dual AGNs)
- Dynamical friction drives the two MBH towards the centre of the new galaxy until they form a bound binary
- 3-body interaction with the surrounding stars subsequently shrinks the binary to pc separation
- How to get them to the millipc separation necessary for GW emission and merger within one Hubble time? **“LAST PARSEC PROBLEM”**
- maybe more stars arrive, or there is gas drag from interaction with a circumbinary disk, and/or another MBH arrives...

If PTAs observe the SGWB from SMBHBs it means that SMBHBs exist and merge in the universe!





# Pulsar timing arrays

Prediction from SMBHBs  
formation scenarios

How does the SGWB from SMBHBs look like?

Characteristic strain:  
red spectrum

$$h_c(f) = A \left( \frac{f}{f_{\text{ref}}} \right)^{-\alpha} \text{ with } \alpha = \frac{2}{3} \quad A = \mathcal{O}(10^{-15}) \text{ at } f_{\text{ref}} = 1 \text{ yr}^{-1}$$

Timing residuals power  
spectral density:  
Also red spectrum

$$S_{ab}(f) = \mathcal{C}(\theta_{ab}) \Phi(f)$$

Circular binary

$$\Phi(f) = \frac{A^2}{(2\pi)^2} f_{\text{ref}}^{-3} \left( \frac{f}{f_{\text{ref}}} \right)^{-\gamma} \text{ with } \gamma = 2\alpha + 3 = \frac{13}{3}$$

The features of the SGWB power spectrum (amplitude  $A$ , slope  $\alpha$ ...) depend on the population characteristics such as the binary merger rate, its dependence with mass and redshift, the surrounding stellar density, the initial binary eccentricity...

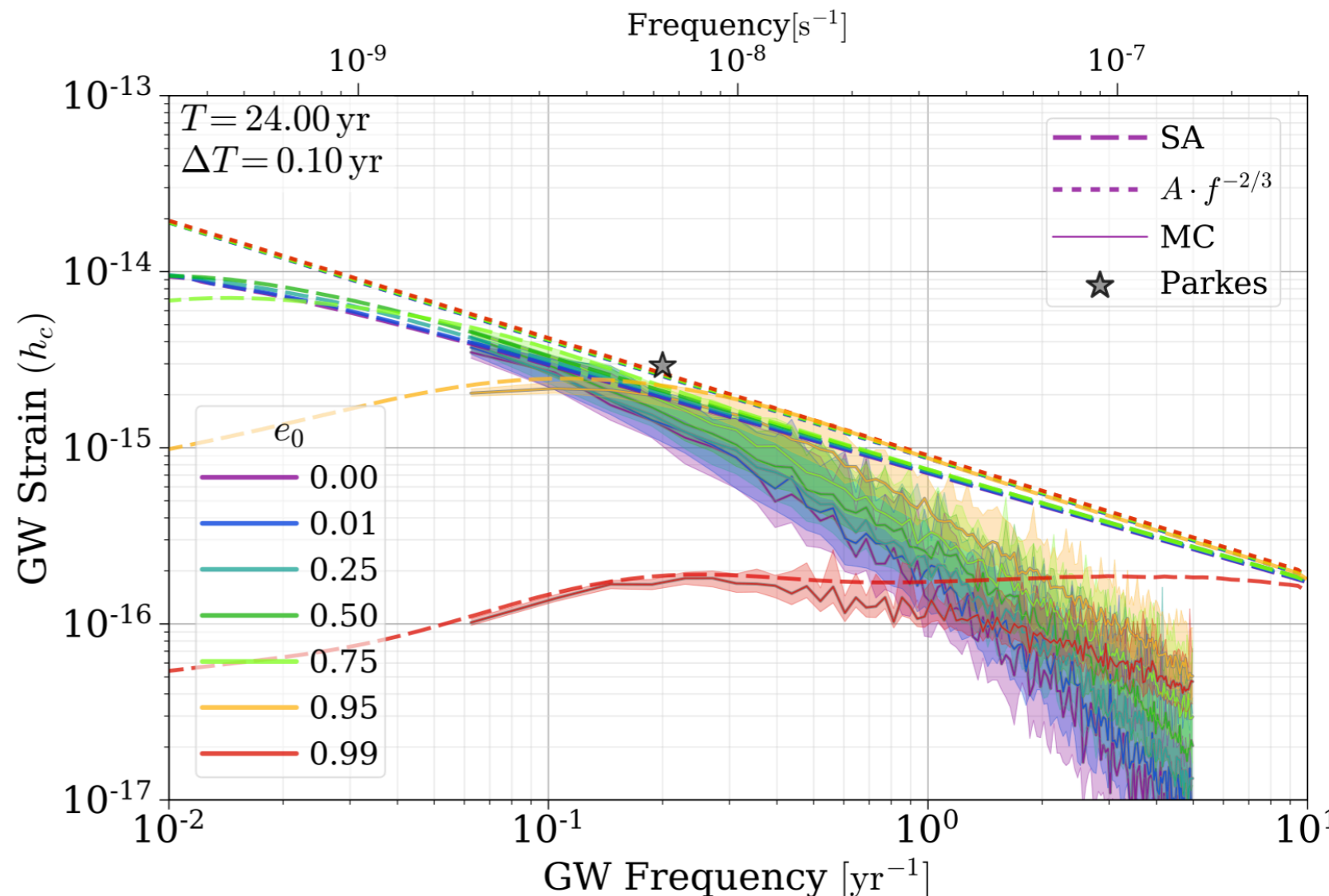
# Pulsar timing arrays

How does the SGWB from SMBHBs look like?

Characteristic strain:  
red spectrum  $h_c(f) = A \left( \frac{f}{f_{\text{ref}}} \right)^{-\alpha}$  with  $\alpha = \frac{2}{3}$   $A = \mathcal{O}(10^{-15})$  at  $f_{\text{ref}} = 1 \text{ yr}^{-1}$

- The assumption of homogeneous and isotropic SGWB isn't justified at high frequency: SMBHBs are less numerous, the SGWB slope is steeper, and discreteness starts to appear with spikes due to the loudest SMBHBs
- Interactions with the binary environment makes hardening stronger and suppresses SGWB power at low frequency
- Eccentricity enhances GW emission at higher frequencies

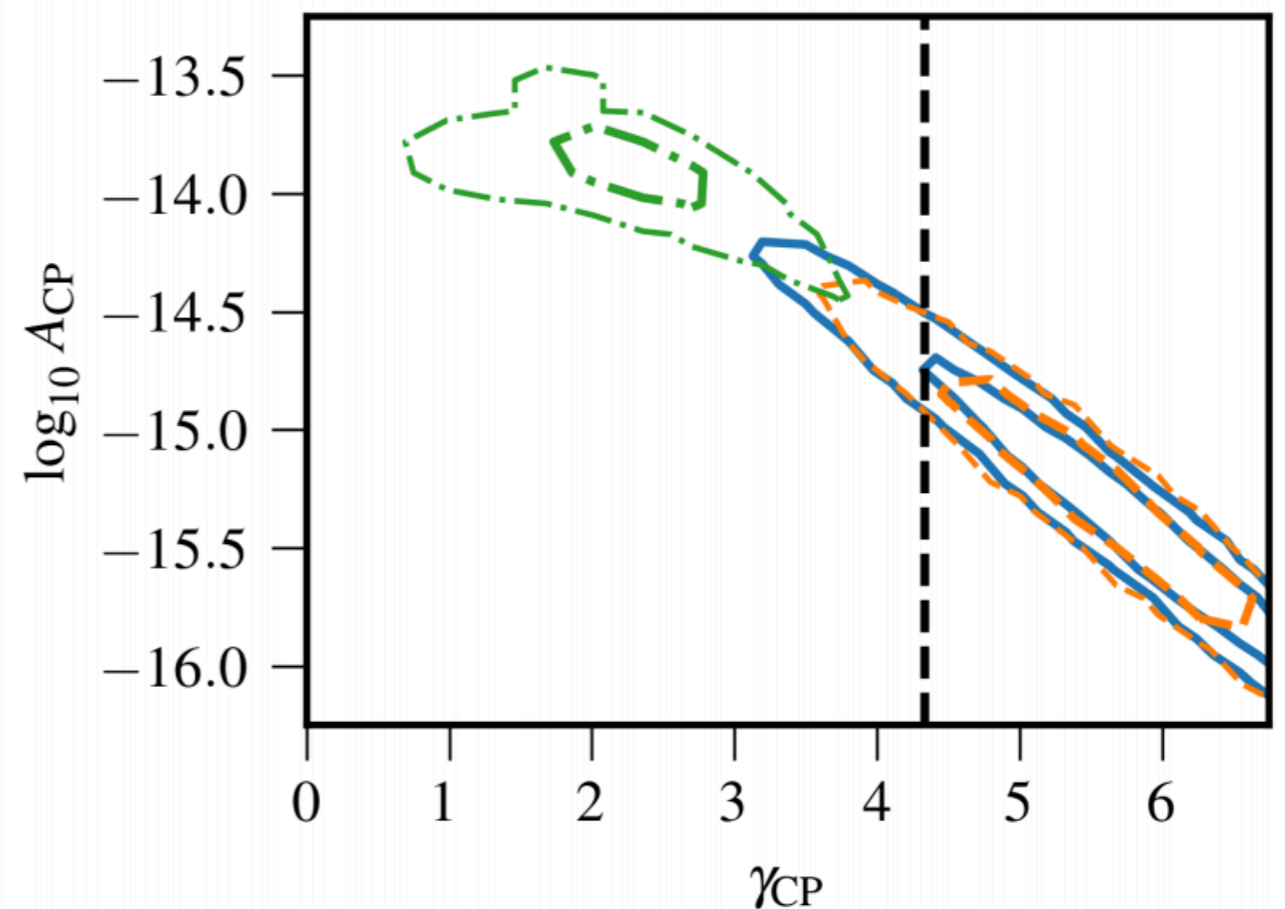
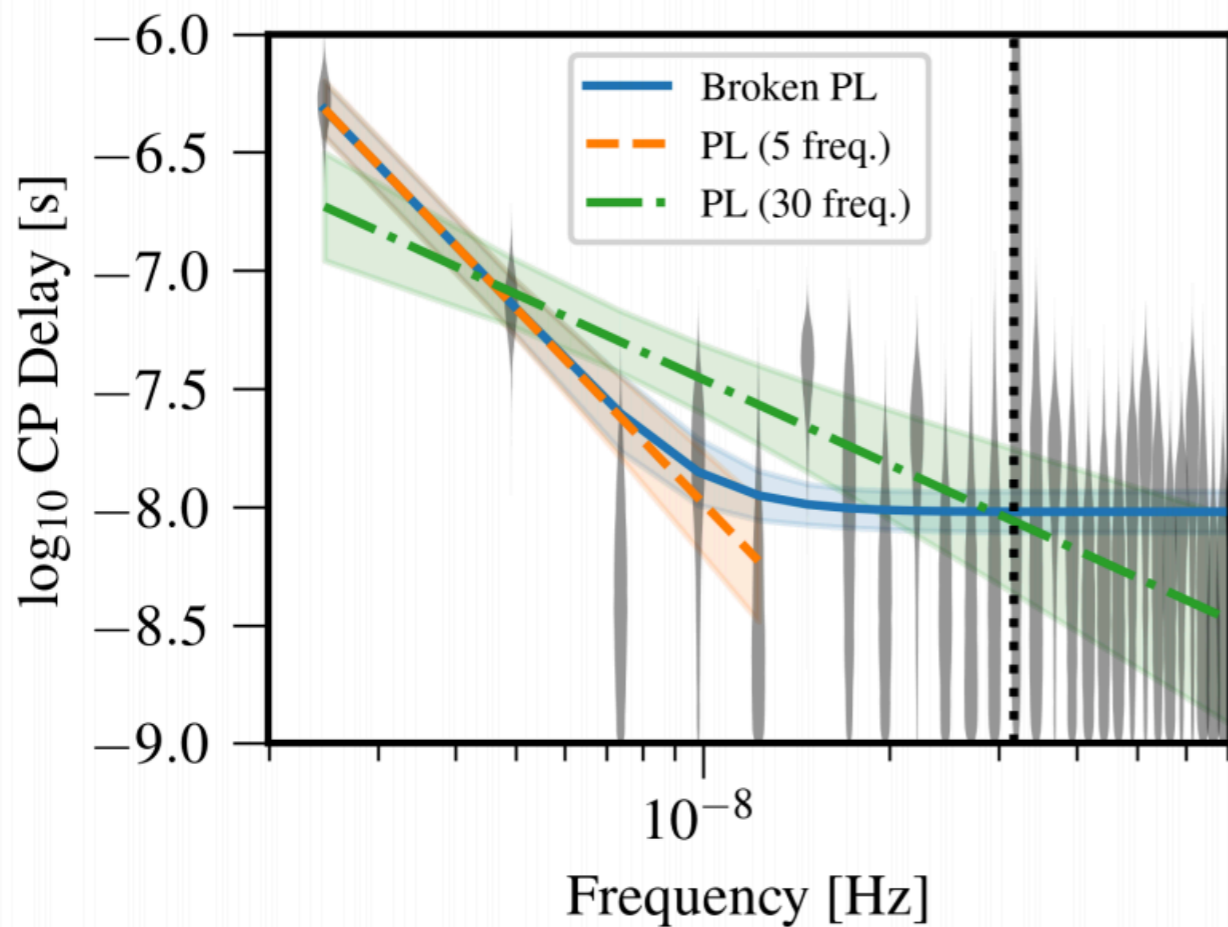
L.Z. Kelley et al, arXiv:1702.02180



# Pulsar timing arrays

In 2020, NANOGrav (followed by EPTA and PPTA) has announced the presence of a common red noise in their 12.5 years data

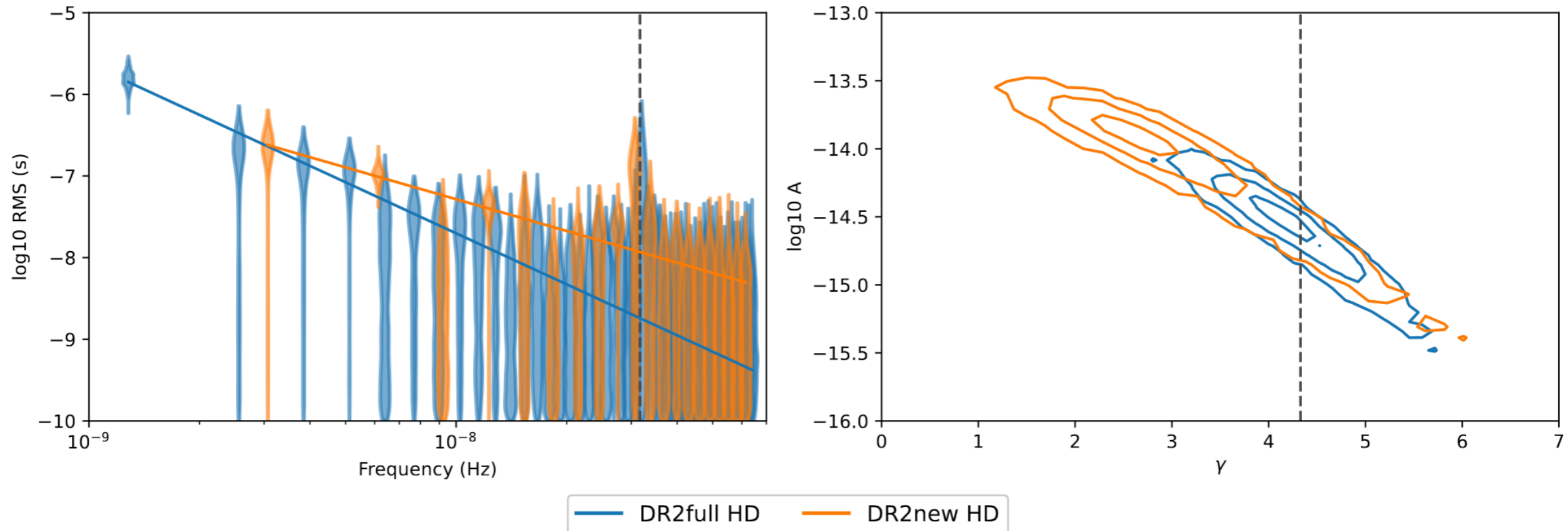
$$\Phi(f) = \frac{A^2}{(2\pi)^2} f_{\text{ref}}^{-3} \left( \frac{f}{f_{\text{ref}}} \right)^{-\gamma} \quad \text{with} \quad \gamma = 2\alpha + 3 = \frac{13}{3}$$



# Pulsar timing arrays

Last year, all PTAs have confirmed the observation of a common red noise supplemented by evidence for the Hellings-Downs correlation

**EPTA  
results:**

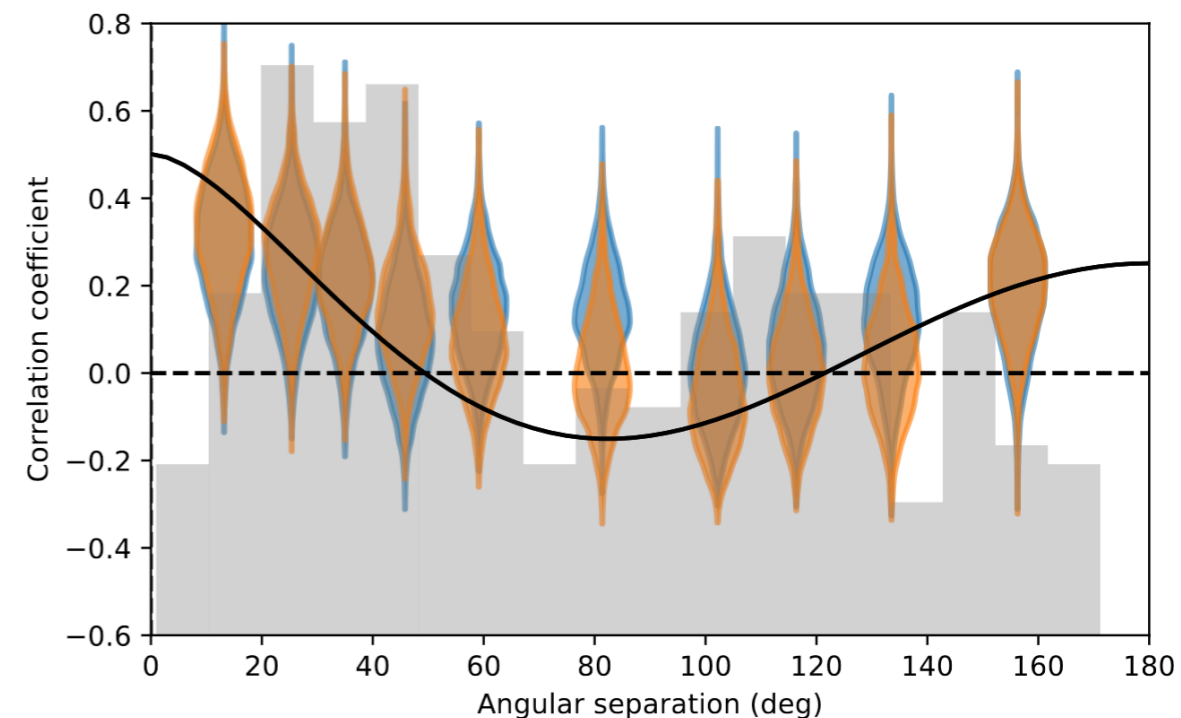


DR2new (10.3 yrs):

$$\log A = -13.94^{+0.23}_{-0.48} \quad \gamma = 2.71^{+1.18}_{-0.73} \quad \mathcal{B} = 60$$

DR2full (25 yrs):

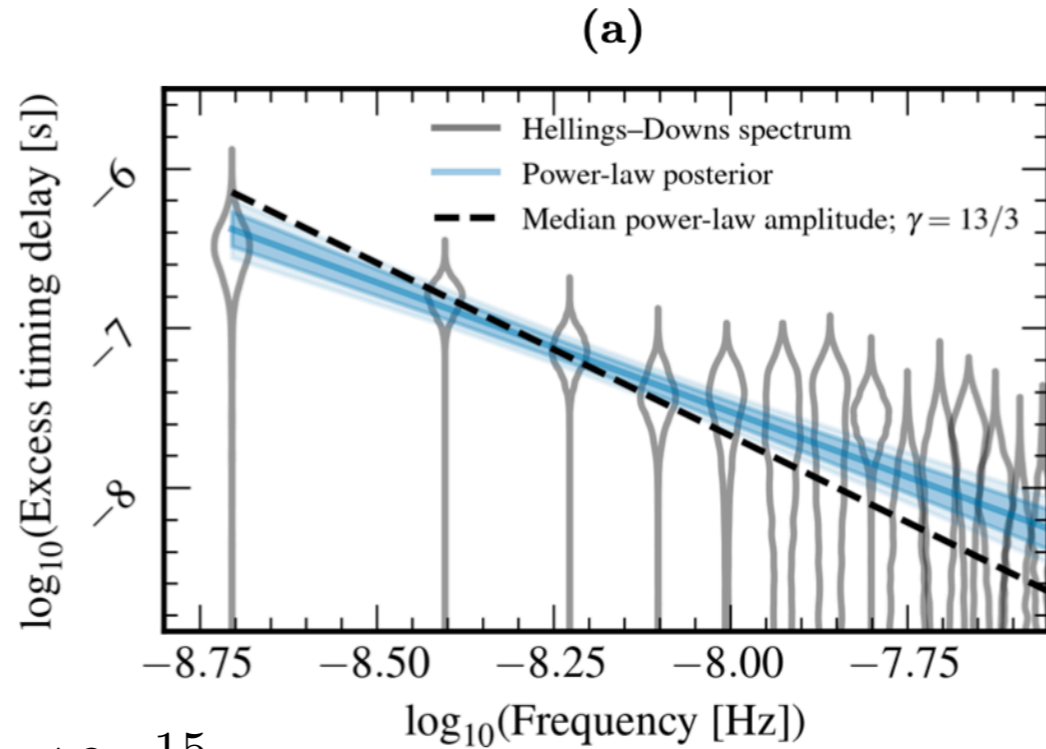
$$\log A = -14.54^{+0.28}_{-0.41} \quad \gamma = 4.19^{+0.73}_{-0.63} \quad \mathcal{B} = 4$$



# Pulsar timing arrays

Last year, all PTAs have confirmed the observation of a common red noise supplemented by evidence for the Hellings-Downs correlation

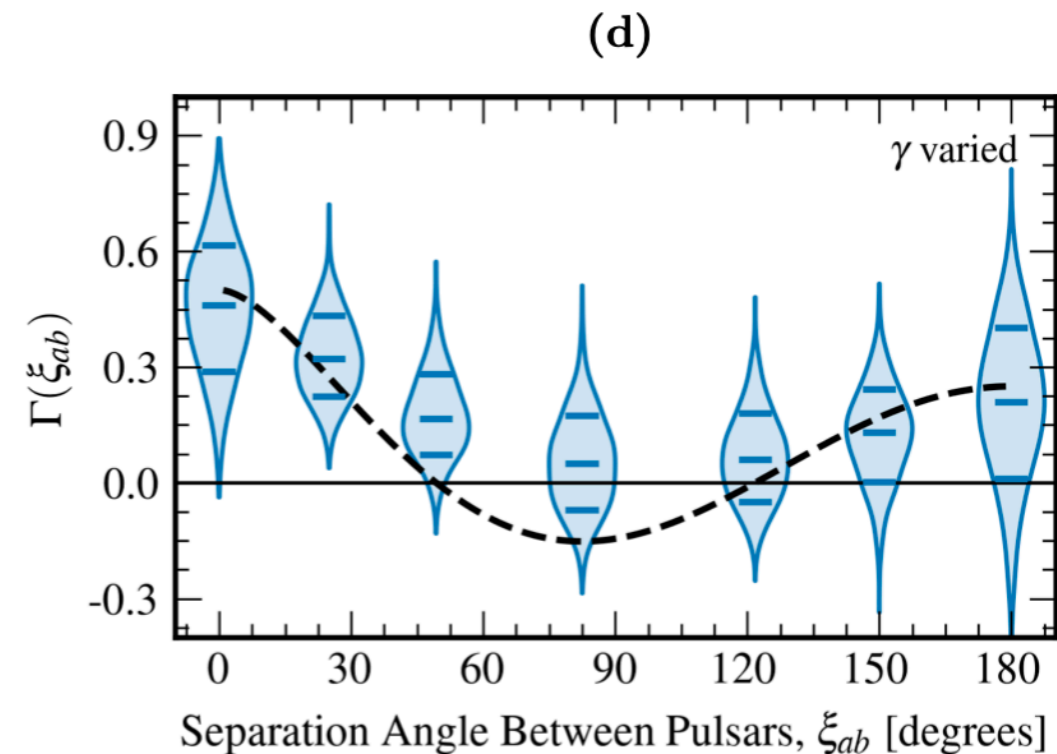
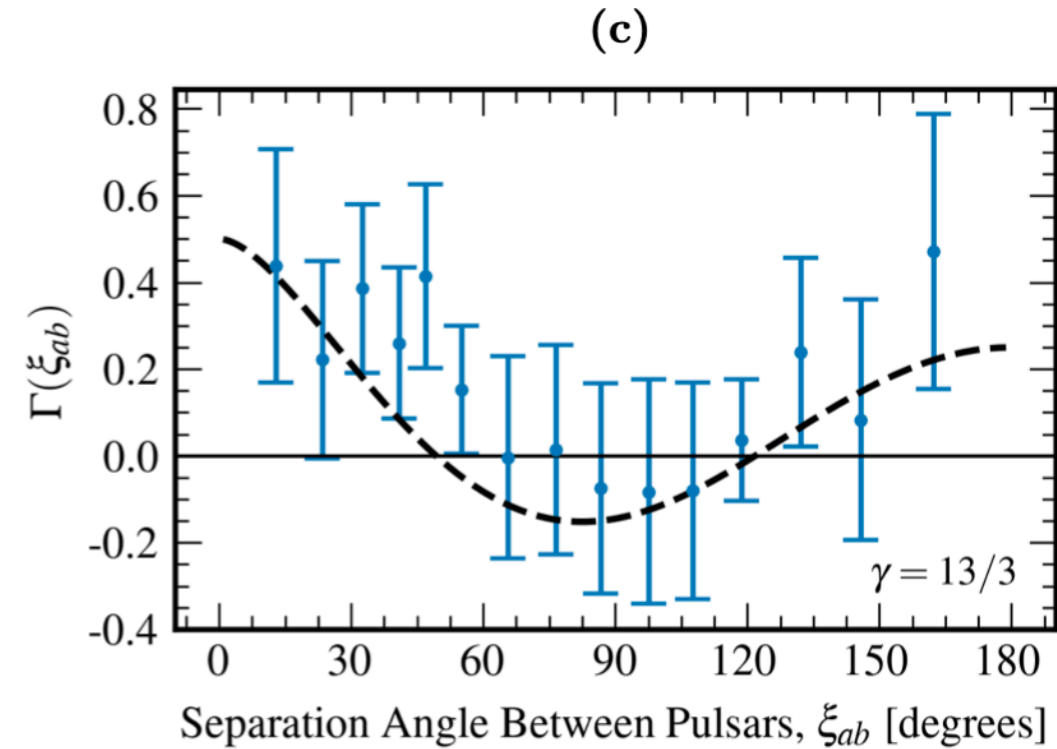
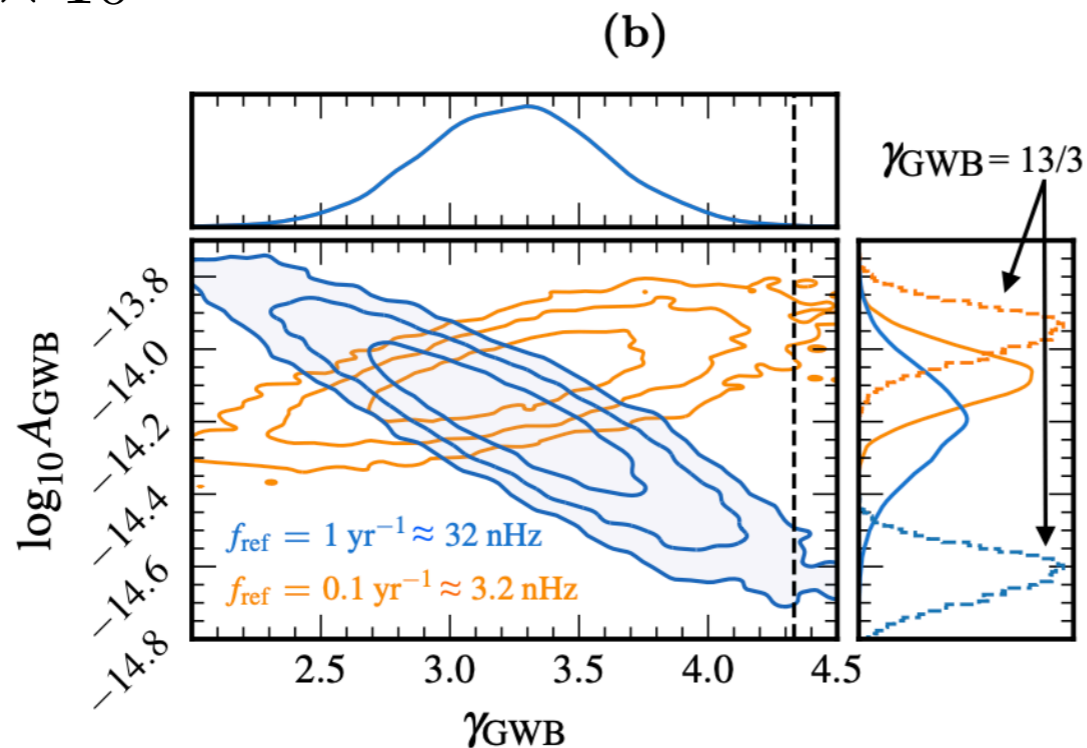
## NANOGrav results:



$$A = -6.4^{+4.2}_{-2.7} \times 10^{-15}$$

$$\gamma = 3.2^{+0.6}_{-0.6}$$

$$B = 226$$

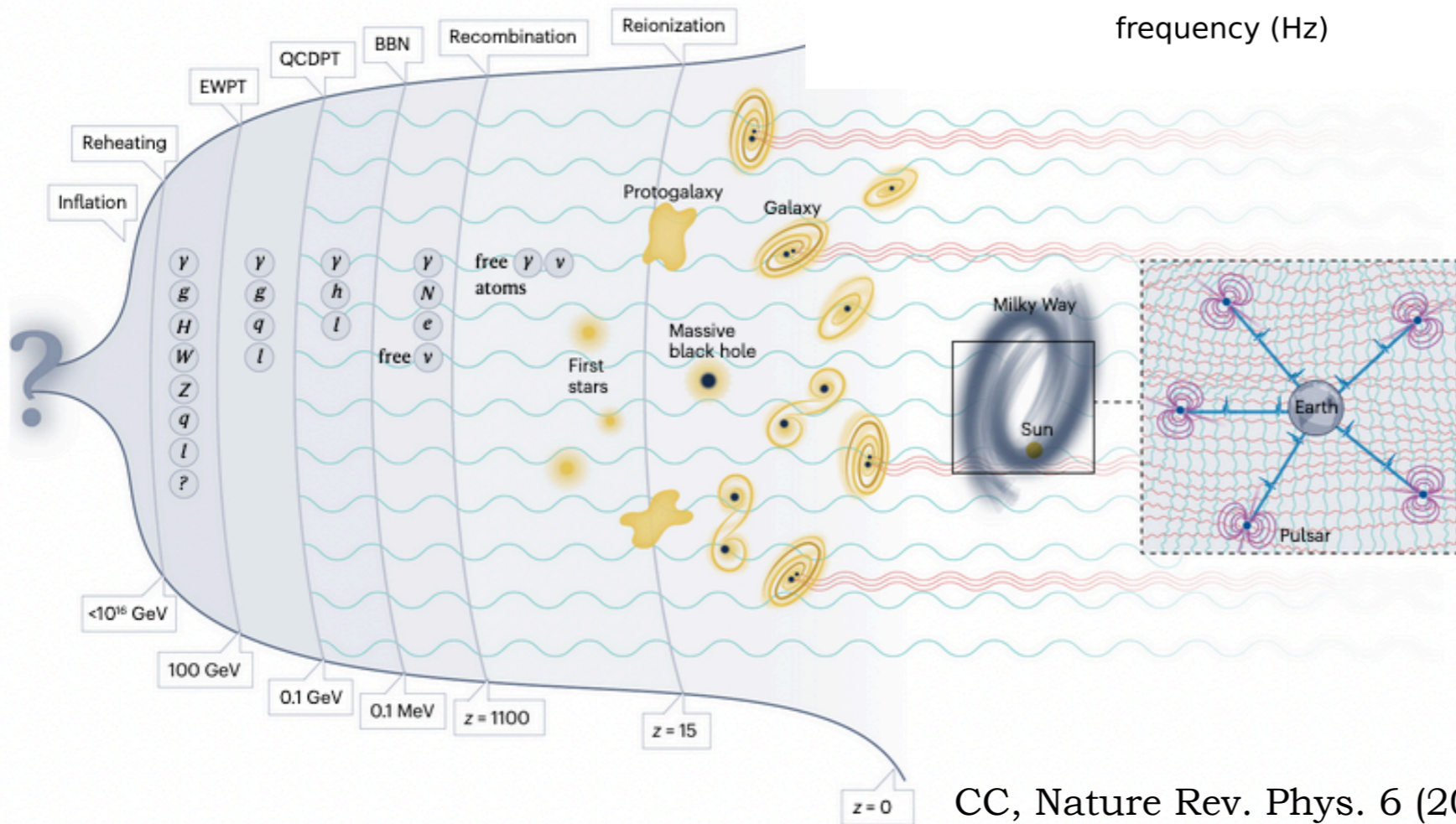
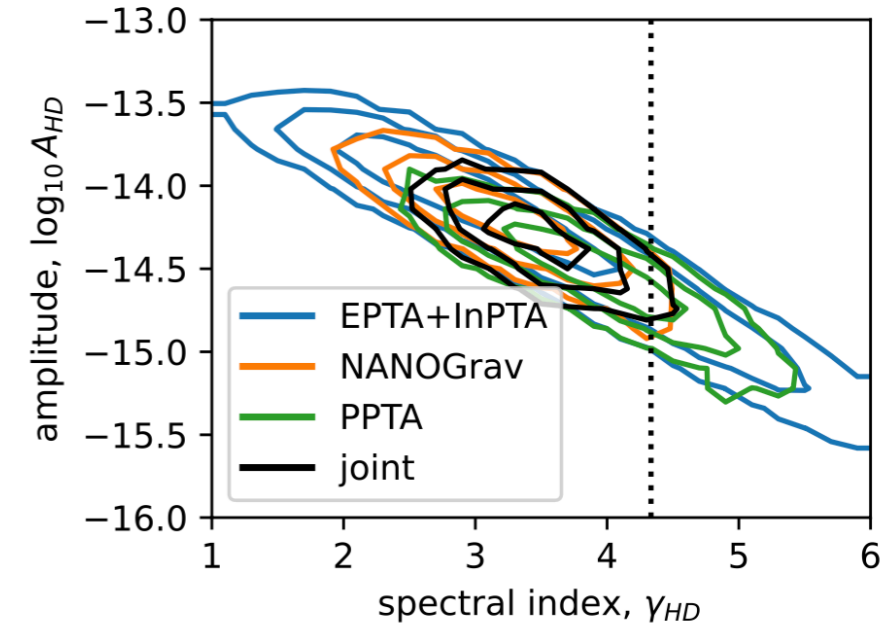
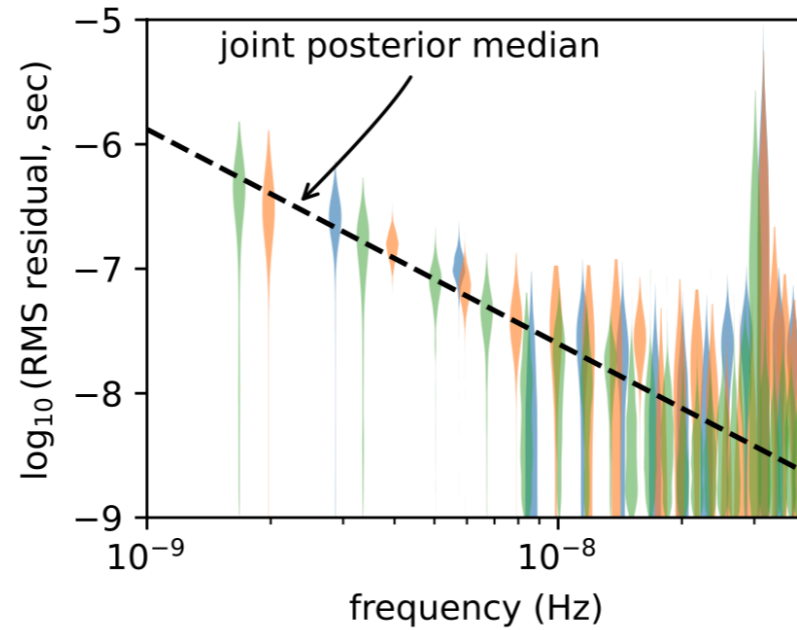




# Pulsar timing arrays

- The slopes are shallower than 13/3 (but maybe the model isn't fully adapted...)
- The amplitude is consistent with the one from a SMBHBs SGWB
- All datasets are consistent within  $1\sigma$  as shown by IPTA

IPTA Collaboration,  
arXiv:2309.00693



But the signal could also be of primordial origin...